Robust Multi-Objective Optimization for EE-SE Tradeoff in D2D Communications Underlaying Heterogeneous Networks

Yuanyuan Hao, Qiang Ni, *Senior Member, IEEE*, Hai Li, *Member, IEEE*, and Shujuan Hou

***Abstract*— In this paper, we concentrate on the robust multi-objective optimization (MOO) for the tradeoff between energy efficiency (EE) and spectral efficiency (SE) in device-to-device (D2D) communications underlaying heterogeneous networks (HetNets). Different from traditional resource optimization, we focus on finding robust Pareto optimal solutions for spectrum allocation and power coordination in D2D communications underlaying HetNets with the consideration of interference channel uncertainties. The problem is formulated as an uncertain MOO problem to maximize EE and SE of cellular users (CUs) simultaneously while guaranteeing the minimum rate requirements of both CUs and D2D pairs. With the aid of ε-constraint method and strict robustness, we propose a general framework to transform the uncertain MOO problem into a deterministic single-objective optimization problem. As exponential computational complexity is required to solve this highly non-convex problem, the power coordination and the spectrum allocation problems are solved separately, and an effective two-stage iterative algorithm is developed. Finally, simulation results validate that our proposed robust scheme converges fast and significantly outperforms the non-robust scheme in terms of the effective EE-SE tradeoff and the quality of service satisfying probability of D2D pairs.**

***Index Terms*— D2D communications, energy efficiency, HetNets, power coordination, robust multi-objective optimization, spectral efficiency, spectrum allocation.**

I. Introduction

With the proliferation of smart mobile services and the intrinsic spectrum scarceness, improving spectral efficiency (SE) has been widely treated as an essential target for the next decade [1]. At the same time, green communications have caught considerable attention, because of explosively rising energy consumption of mobile networks and corresponding environmental concerns [2]. Therefore, the enhancement of energy efficiency (EE) is another key objective for the future fifth-generation (5G) networks [3]. To tackle these difficulties, there is a general consensus that dense network deployment will play an important role, such as multi-tier heterogeneous networks (HetNets) and device-to-device (D2D) communications, especially when employed in combination [4].

D2D communications enable wireless point-to-point services directly between two mobile devices as well as offload the traffic of cellular base stations (BSs), which contribute to the improvement of the network EE and SE due to high spectral utilization and the physical proximity between D2D pairs [5], [6]. On the other hand, the multi-tier HetNet has been identified as a promising network architecture for 5G to drastically improve EE and SE [7]–[9], as multiple small cells share the same spectrum with each macro cell which promotes the dense spectrum reuse. Based on the above observation, the study on the D2D communications underlaying HetNets is indeed of vital importance because of the expected heterogeneous nature of the future 5G networks. For multi-tier HetNets operating with universal frequency reuse, cross-tier and co-tier interference are the main challenges [10], and extra interference is imposed when underlaid D2D communications are admitted. As a consequence, in D2D communications underlaying HetNets, spectrum allocation and power coordination mechanisms are more complicated in comparison with those in traditional homogeneous cellular networks, and they are essential to achieve the potential benefits from D2D communications and multi-tier HetNets.

A. Related Work

There have been numerous studies about the energy efficient resource allocation for D2D communications [11]–[20]. In [11], Xu *et al.* focus on optimizing the energy consumption of the BS in D2D communications underlying cellular networks by optimally coordinating users to redistribute the traffic, while Fodor *et al.* [12] investigate the performance of various power control strategies for D2D communications in LTE networks. Furthermore, considering the simple system with one D2D link and one cellular user (CU), the work in [13] proposes an extended binary power control method to maximize the utility which balances SE and power. Wu *et al.* [14] also consider the scenario with single D2D link and single CU, where the D2D user's EE is optimized

Manuscript received November 21, 2017; revised March 6, 2018 and May 2, 2018; accepted May 3, 2018. Date of publication May 10, 2018; date of current version October 16, 2018. This work was supported in part by the EPSRC IAA project CSA7114, EPSRC project EP/K011693/1 and EU CROWN project under grant PIRSES-GA-2013-610524. The editor coordinating the review of this paper and approving it for publication was M. Di Renzo. *(Corresponding author: Shujuan Hou.)*

Y. Hao, H. Li, and S. Hou are with the School of Information and Electronics, Beijing Institute of Technology, Beijing 100081, China (e-mail: tracyhao@bit.edu.cn; haili@bit.edu.cn; shujuanhou@bit.edu.cn).

Q. Ni is with the School of Computing and Communications, Lancaster University, Lancaster LA1 4WA, U.K. (e-mail: q.ni@lancaster.ac.uk).

Digital Object Identifier 10.1109/TCOMM.2018.2834920

under the minimum rate constraints of both CU and D2D users. Similarly, in [15], the resource allocation problem for underlay or overlay D2D communications and cognitive radio systems is formulated as the maximization of the secondary energy efficiency subject to a minimum rate requirement for the primary user, where a sequential optimization method is proposed. Recently, Penda *et al.* [16] investigate the problem of minimizing the transmission energy consumption while satisfying a traffic requirement for D2D communications in a single-cell network. In [17], Jiang *et al.* consider the joint resource allocation and power control problem which aims at maximizing the EE of all D2D links. Instead, the work in [18] focuses on maximizing the minimum weighted EE of D2D pairs under the minimum rate requirements of cellular users, while Wu *et al.* [19] formulate the energy-efficient resource sharing problem in D2D communications underlaying cellular networks as a nontransferable coalition formation game. Besides, Yang *et al.* [20] investigate energy efficient power control in D2D communications underlaying cellular networks, where both the system EE and individual EE optimization problems are considered.

Nevertheless, the above studies [11]–[20] consider D2D communications underlaying or overlaying single-tier networks, and the research on resource allocation in D2D communications underlaying HetNets is still limited. In [21], Asheralieva *et al.* consider the channel and power level selection problem for D2D pairs in HetNets under two scenarios where D2D pairs operate over the dedicated frequency band and the shared cellular channels, which is formulated as a non-cooperative game among D2D pairs. Besides, the work in [22] investigates the resource allocation problem to maximize the system secure capacity for D2D communications underlaying HetNets where each subcarrier can be allocated to at most one user of the same type. On the contrary, Alqerm and Shihada [23] focus on the power allocation problem in multi-tier HetNets by employing a non-cooperative scheme to optimize the individual EE of each small cell BS and each D2D pair.

However, either EE or SE is neglected in the aforementioned work [11]–[23]. There have been studies about the joint optimization of EE and SE for D2D communications in single-cell networks [24], [25] and for HetNets [26]. As EE and SE potentially conflict with each other such that available resource cannot be optimized to improve both EE and SE simultaneously, it is indispensable to investigate the tradeoff between EE and SE for D2D communications underlaying HetNets, which can provide decision makers with the entire performance envelop of EE and SE. More importantly, in all the previous studies [11]–[26], it is assumed that perfect channel state information (CSI) is available, while this assumption cannot be achieved in practical scenarios. Due to the random nature of wireless channels, limited capacity and transmission delay of backhaul channels, and inaccurate channel estimation, the CSI inevitably contains errors, which may substantially deteriorate the system performance. Particularly, for D2D communications underlaying HetNets, the QoS requirements of cellular users (CUs) and D2D pairs cannot be strictly satisfied when channel uncertainties exist.

To address the uncertainties of CSI, robust optimization has been studied in wireless communications [27]–[29]. In [27], two robust resource allocation schemes for cognitive radio networks are developed to maximize the system goodput while satisfying the interference constraints of primary user for probabilistic and bounded channel uncertainty model, respectively. Memmi *et al.* [28] propose centralized and distributed power control algorithms for D2D underlay cellular networks where the CSI includes estimation errors. Similarly, considering interference channel uncertainties, the work in [29] focuses on the uplink resource allocation algorithm in relay-aided D2D communications with the help of worst case optimization method. However, all the studies in [27]–[29] focus on robust single-objective optimization problem (RSOP), and the effect of channel uncertainties on the multi-objective optimization problem is still unknown.

B. Contributions

As far as we know, there is no existing study about the EE-SE tradeoff in D2D communications underlaying HetNets with universal frequency reuse among macro BSs, pico BSs and D2D pairs. Also, considering channel uncertainties, the research on robust multi-objective optimization problem (RMOP) is still missing. Inspired by these facts, in this paper, we investigate the RMOP for D2D communications underlaying HetNets. To mitigate the negative effects of underlaid D2D communications on the primary HetNets while strictly ensuring the minimum rate requirements of D2D pairs, the RMOP is formulated as maximizing the EE and SE of CUs while strictly ensuring the minimum rate requirements of both CUs and D2D pairs, where the spectrum allocation and power coordination of CUs and D2D users are jointly optimized. Specifically, the main contributions are given as follows:

- This is the first work which models the robust multi-objective optimization problem to investigate the tradeoff between EE and SE in D2D communications underlaying HetNets while considering interference channel uncertainties. Specifically, the problem is formulated as an uncertain MOO problem which maximizes the sum rate of all CUs and minimizes the corresponding total power consumption simultaneously while strictly ensuring the minimum rate requirements of both CUs and D2D pairs.
- To find the optimal solutions of the formulated uncertain MOO problem, we propose a general framework which transforms the uncertain MOO problem into a deterministic SOO problem, with the help of ε-constraint method and strict robustness. Crucially, it is demonstrated theoretically that the unique optimal solution of the deterministic SOO problem is *robust Pareto optimal* for the original uncertain MOO problem. Consequently, the proposed framework is guaranteed to find all robust Pareto optimal solutions of the formulated uncertain MOO problem, i.e., robust Pareto frontier is obtained.
- The spectrum allocation for D2D pairs and the power coordination of CUs and D2D pairs are jointly optimized in D2D communications underlaying HetNets, which is

a mixed-integer and non-convex problem due to the intrinsic integer property of resource block (RB) allocation and the existence of mutual interference among CUs and D2D pairs sharing the same RB. Thus, we propose a computationally-efficient iterative algorithm where primal decomposition is employed to separate the original problem into two subproblems. To be more specific, the power coordination problem is solved via D. C. (difference of convex functions) programming. On the other hand, we model the spectrum allocation problem as a many-to-one matching game, and propose initial matching and swap matching algorithms.

- The optimality, convergence, and complexity of our proposed methods are presented in detail. Via theoretical analysis, it is proved that our proposed power coordination method and spectrum allocation algorithm converge within a finite number of iterations. Furthermore, the convergence of the overall two-stage iterative algorithm is verified by both theoretical analysis and numerical results, and its whole computational complexity is also given in detail. More importantly, it is demonstrated via numerical results that our proposed robust scheme significantly outperforms the non-robust scheme in terms of the effective EE-SE tradeoff and the quality of service (QoS) satisfying probability of D2D pairs. Particularly, through numerical results, we find that there exists an intrinsic tradeoff between the EE-SE performance of CUs and the minimum rate requirements of D2D pairs. Besides, it is suggested that the choice of the maximum number of D2D pairs on each RB should be appropriate for the compromise between complexity and performance gain.

C. Paper Organization

The remainder of this paper is organized as below. The system model and the nominal problem formulation are first presented in Section II. Then, in Section III, the uncertain MOO problem is formulated and transformed into a deterministic SOO problem, and we propose effective algorithms for the joint optimization of power coordination and spectrum allocation in Section IV. Finally, numerical results and conclusions are given in Section V and Section VI, respectively.

II. System Model and Deterministic Problem Formulation

We consider a D2D communications underlaying HetNet, which is shown in Fig. 1, composed of a macro base station (MBS), I pico BSs (PBSs), N CUs, and K D2D pairs. Let $\mathcal{C} = \{1, 2, \cdots, N\}$ denote the set of CUs, and the indexes of D2D pairs are given by $k \in \mathcal{D} = \{1, 2, \cdots, K\}$. We use $i \in \{0, 1, 2, \cdots, I\}$ as the indexes of BSs, where $i = 0$ corresponds to the MBS, and the others are PBSs. Besides, we assume that the spectrum is shared by all BSs, and orthogonal frequency-division multiple access (OFDMA) is adopted for CUs associated with the same BS, which is predetermined. Let $\mathcal{M} = \{1, 2, \cdots, M\}$ denote the set of resource blocks (RBs) for uplink transmission, and $\mathcal{M}_n^{\mathrm{C}}$ is used to indicate the set of RBs which are occupied by the n-th CU. We assume that each RB can be reused by multiple D2D pairs. Consequently, there exists not only inter-cell interference among CUs associated with different BSs, but also mutual interference among CUs and D2D pairs sharing the same RB.

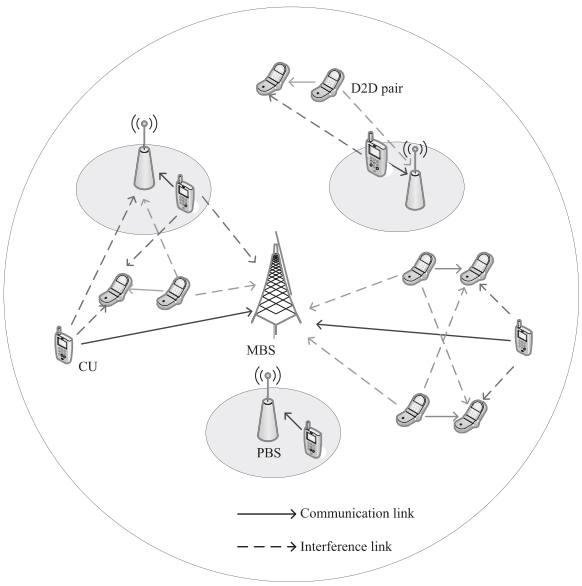

Fig. 1. System model.

A. Transmission Data Rate

We first introduce p_{nm}^{C} to represent the transmit power of the n-th CU on the m-th RB, and p_k^{D} denotes the transmit power of the k-th D2D pair. Then, let ρ_{km} describe the m-th RB allocation for the k-th D2D pair, where $\rho_{km} = 1$ if RB-m is allocated to the k-th D2D pair, $\rho_{km} = 0$, otherwise. Thus, the transmission data rate of CU-n associated with the i-th BS can be expressed as

$$R_n^{\mathrm{C}} = \sum_{m \in \mathcal{M}_n^{\mathrm{C}}} \log_2 \left(1 + \frac{p_{nm}^{\mathrm{C}} h_{ni}^m}{I_{nm}^{\mathrm{C}} + \sigma^2}\right), \tag{1}$$

where h_{ni}^m is the channel power gain between the n-th CU and the i-th BS on the m-th RB, and $I_{nm}^{\mathrm{C}} = \sum_{n' \in \mathcal{C}_m, n' \neq n} p_{n'm}^{\mathrm{C}} g_{n'i}^m + \sum_{k \in \mathcal{D}} \rho_{km} p_k^{\mathrm{D}} g_{ki}^m$ denotes the interference experienced by CU-n on the m-th RB. $g_{n'i}^m$ and g_{ki}^m represent the interference channel power gains from other CUs and D2D pairs sharing the m-th RB. Note that $\mathcal{C}_m$ represents the set of CUs who transmit data on the m-th RB. Similarly, the transmission data rate of the k-th D2D pair can be calculated by

$$R_k^{\mathrm{D}} = \sum_{m \in \mathcal{M}} \rho_{km} \log_2 \left(1 + \frac{p_k^{\mathrm{D}} h_k^m}{I_{km}^{\mathrm{D}} + \sigma^2}\right), \tag{2}$$

where h_k^m denotes the channel power gain of the k-th D2D pair on the m-th RB, and $I_{km}^{\mathrm{D}} = \sum_{n \in \mathcal{C}_m} p_{nm}^{\mathrm{C}} g_{nk}^m + \sum_{j \in \mathcal{D}, j \neq k} \rho_{jm} p_j^{\mathrm{D}} g_{jk}^m$ is the interference received by the k-th D2D pair on RB-m.

g_{nk}^m and g_{jk}^m represent the interference channel power gains from the *n*-th CU and the *j*-th D2D pair, respectively.

B. SE and EE

In this paper, we define the system SE (bit/s/Hz) as the sum transmission rate of all CUs per unit bandwidth, which can be expressed as

$$\eta_{\mathrm{SE}} = R_{\mathrm{tot}} = \sum_{n\in\mathcal{C}} R_n^{\mathrm{C}}. \tag{3}$$

Furthermore, the system EE (bit/Joule/Hz) is stated as the ratio of the system SE to the corresponding power consumption, which is presented as

$$\eta_{\mathrm{EE}} = \frac{\eta_{\mathrm{SE}}}{P_{\mathrm{tot}}} = \frac{\sum\limits_{n\in\mathcal{C}} R_n^{\mathrm{C}}}{\frac{1}{\alpha}\sum\limits_{n\in\mathcal{C}}\sum\limits_{m\in\mathcal{M}_n^{\mathrm{C}}} p_{nm}^{\mathrm{C}} + Np_{\mathrm{s}}}. \tag{4}$$

Here α denotes the transmit amplifier efficiency, and p_{s} represents the fixed circuit power consumption of each CU.

III. Robust Multi-Objective Optimization for EE-SE Tradeoff

In this section, we first present the nominal MOO problem for the EE-SE tradeoff in D2D communication underlaying HetNets, where perfect CSI is assumed. Then, with the consideration of channel uncertainty, robust MOO problem is further formulated and transformed into a deterministic SOO problem to facilitate problem solving.

A. Problem Formulation: Nominal Multi-Objective Optimization

It has been widely recognised that EE and SE conflict with each other for a communication system with fixed radio resources [30], [31]. Hence, the individual maximization of EE or SE cannot always meet the system performance requirement, and it is significant to study the tradeoff between EE and SE and present the whole performance envelop of EE and SE. In fact, the EE-SE tradeoff problem is equivalent to a set of problems of finding the maximum EE with different fixed SE [25]. Furthermore, as EE is the ratio between SE and the total power consumption as shown in (4), for the same SE, the minimization of power is equivalent to the maximization of EE. Therefore, the joint optimization of EE and SE can be achieved by maximizing SE and minimizing the total power consumption simultaneously. Besides, as illustrated in [32], both the EE maximization and the SE maximization problems can be captured by the multi-objective optimization problem of maximizing SE and minimizing the total power consumption simultaneously. Thus, the joint optimization of power coordination and spectrum allocation for the tradeoff between EE and SE in D2D communications underlaying HetNets can be formulated as a MOO problem, which can be expressed as

$$\begin{aligned}
&\min_{\boldsymbol{\rho},\mathbf{p}^{\mathrm{C}},\mathbf{p}^{\mathrm{D}}} \ \mathrm{f}_1\left(\boldsymbol{\rho},\mathbf{p}^{\mathrm{C}},\mathbf{p}^{\mathrm{D}}\right) = -\sum_{n\in\mathcal{C}} R_n^{\mathrm{C}},\\
&\min_{\boldsymbol{\rho},\mathbf{p}^{\mathrm{C}},\mathbf{p}^{\mathrm{D}}} \ \mathrm{f}_2\left(\boldsymbol{\rho},\mathbf{p}^{\mathrm{C}},\mathbf{p}^{\mathrm{D}}\right) = \alpha\sum_{n\in\mathcal{C}}\sum_{m\in\mathcal{M}_n^{\mathrm{C}}} p_{nm}^{\mathrm{C}} + Np_{\mathrm{s}},\\
&\text{s.t. } \mathrm{C1}: \rho_{km}\in\{0,1\}, \quad \forall k\in\mathcal{D},\ m\in\mathcal{M},\\
&\qquad \mathrm{C2}: \sum_{m\in\mathcal{M}}\rho_{km} = 1, \quad \forall k\in\mathcal{D},\\
&\qquad \mathrm{C3}: \sum_{k\in\mathcal{D}}\rho_{km} \le Q, \quad \forall m\in\mathcal{M},\\
&\qquad \mathrm{C4}: \sum_{m\in\mathcal{M}_n^{\mathrm{C}}} p_{nm}^{\mathrm{C}} \le p_{\max}^{\mathrm{C}}, \quad \forall n\in\mathcal{C},\\
&\qquad \mathrm{C5}: p_k^{\mathrm{D}} \le p_{\max}^{\mathrm{D}}, \quad \forall k\in\mathcal{D},\\
&\qquad \mathrm{C6}: R_n^{\mathrm{C}} \ge R_{n,\min}^{\mathrm{C}}, \quad \forall n\in\mathcal{C},\\
&\qquad \mathrm{C7}: R_k^{\mathrm{D}} \ge R_{k,\min}^{\mathrm{D}}, \quad \forall k\in\mathcal{D},
\end{aligned} \tag{5}$$

where $p_{\max}^{\mathrm{C}}$ and $p_{\max}^{\mathrm{D}}$ denote the maximum transmit power of CUs and D2D pairs, respectively. In (5), C1 and C2 denote that each D2D pair can only use one RB for data transmission. C3 indicates that at most Q D2D pairs share the same RB with one CU. In other words, the quota of each RB is set to Q. Then, C4 and C5 mean that the transmit power of CUs and the transmitters of D2D pairs cannot exceed their maximum limits. C6 and C7 ensure the minimum data rates of CUs and D2D pairs, respectively.

Remark 1 (Virtual D2D Pairs for Extended Systems): As shown in problem (5), each D2D pair can only use one RB for data transmission. To generalize the proposed formulation to fit the extended system where each D2D pair can utilize multiple RBs and each RB can be occupied by multiple D2D pairs, we introduce the idea of virtual D2D pairs. Specifically, when the minimum rate requirement of the *k*-th D2D pair $R_{k,\min}^{\mathrm{D}}$ is large for certain applications and multiple RBs are required for data transmission, its rate requirement can be splited into $R_{k,\min}^{\mathrm{D}}/v_k$ by introducing $v_k - 1$ virtual D2D pairs. With the help of new introduced virtual D2D pairs each of which occupies one RB, the original *k*-th D2D pair can utilize multiple RBs simultaneously.[1]

In contrast to the SOO problem, the MOO problem (5) considers two conflicting objectives simultaneously. In such case, there is no single global optimal solution but it is often necessary to determine a set of alternatives that all fit a predetermined definition for an optimum, called *Pareto optimality* [33].

Definition 1 (Pareto Optimality): For a multi-objective optimization problem,

$$\begin{aligned}
&\min_{\mathbf{x}} \ \mathrm{F}(\mathbf{x}) = \left[\mathrm{f}_1(\mathbf{x})\,\mathrm{f}_2(\mathbf{x})\cdots\mathrm{f}_O(\mathbf{x})\right]^{\mathrm{T}},\\
&\text{s.t. } \mathbf{x}\in\mathcal{X}
\end{aligned} \tag{6}$$

a point $\mathbf{x}^*\in\mathcal{X}$ is Pareto optimal if and only if (iff) there does not exist another point $\mathbf{x}\in\mathcal{X}$ such that $\mathrm{f}_u(\mathbf{x}) \le \mathrm{f}_u(\mathbf{x}^*), \forall u\in\{1,2,\cdots,O\}$, with at least one $v\in\{1,2,\cdots,O\}$ satisfying $\mathrm{f}_v(\mathbf{x}) < \mathrm{f}_v(\mathbf{x}^*)$.

Furthermore, we define cones $\mathbb{R}_{\ge}^k = \left\{\mathbf{y}\in\mathbb{R}^k, \mathbf{y}\ge\mathbf{0}\right\}$, and $\mathrm{F}(\mathbf{x}^*) - \mathbb{R}_{\ge}^O = \left\{\mathbf{y}\in\mathbb{R}^O, \mathbf{y}\le\mathrm{F}(\mathbf{x}^*)\right\}$. Thus, we have that $\mathbf{x}^*$ is Pareto optimal iff $\mathrm{F}(\mathbf{x}^*) - \mathbb{R}_{\ge}^O$ does not contain any $\mathrm{F}(\mathbf{x})$ with $\mathbf{x}\in\mathcal{X}$. Note that $\mathbf{A}\le\mathbf{B}$ represents that $\mathbf{A}$ is

[1]Note that the specific operations about D2D rate requirement splitting and virtual D2D pairs are not taken into consideration in the rest of this paper and set aside for our future work.

smaller or equal to $\mathbf{B}$ in every component, and smaller in at least one component.

Remark 2: As mentioned before, optimizing problem (5) and finding the corresponding SE-power Pareto frontier can provide decision maker with the entire performance envelope between EE and SE. Nevertheless, as it is non-trivial to find the point corresponding to the maximum EE from the entire Pareto frontier by choosing one appropriate weight, the maximization of EE should be also conducted through problem (5) like [32] to characterize the tradeoff between EE and SE.

B. Problem Formulation: Robust Multi-Objective Optimization

The formulated problem (5) requires perfect interference channel state information (CSI), namely, exact values of $\mathbf{g}^{\mathrm{C2B}} = [g^m_{n'i}]$, $\mathbf{g}^{\mathrm{D2B}} = [g^m_{ki}]$, $\mathbf{g}^{\mathrm{C2D}} = [g^m_{nk}]$, and $\mathbf{g}^{\mathrm{D2D}} = \left[g^m_{jk}\right]$. However, these parameters are subjected to uncertainty, considering the channel estimation errors and the limited capacity of backhaul links. Hence, in this paper, it is assumed that only partial CSI of interference links is available, while perfect CSI of communication links is obtained. Considering the bounded uncertainty [27], we assume that the uncertainty of interference channel gains is bounded and no statistic knowledge is available. Specifically, the interference channel gain can be modelled as $y = \hat{y} + \zeta$, where $|\zeta| \le \zeta_{\max}$ denotes the estimation error. Then, the corresponding power gain can be given by

$$g = |y|^2 = y\bar{y} = (\hat{y} + \zeta)\left(\bar{\hat{y}} + \bar{\zeta}\right) = \hat{g} + \delta, \tag{7}$$

where $\hat{g} = \hat{y}\bar{\hat{y}}$ is the estimated channel power gain, and $\delta = \zeta\bar{\zeta} + 2\Re\left(\hat{y}\bar{\zeta}\right)$ is the estimation uncertainty. Here $\Re(x)$ represents the real component of x. As y lies in a bounded region, the power gain g is in a set of line segment. Here we consider the worst case, and the uncertain region of g can be expressed as

$$g \in \mathcal{R} = \{\hat{g} + \delta : |\delta| \le \delta_{\max}\}, \tag{8}$$

where $\delta_{\max} = \zeta_{\max}\bar{\zeta}_{\max} + 2\Re\left(\hat{y}\bar{\zeta}_{\max}\right)$.

Therefore, the uncertainty region for the inter-cell interference gain from the n'-th CU to the i-th BS on RB-m is presented as

$$g^m_{n'i} \in \mathcal{G}^m_{n'i} = \left\{\hat{g}^m_{n'i} + \delta^m_{n'i} : |\delta^m_{n'i}| \le \delta^m_{n'i,\max}, \forall i, m, n'\right\}. \tag{9}$$

Also, the interference gain between the k-th D2D pair and BS-i on the m-th RB is given by

$$g^m_{ki} \in \mathcal{G}^m_{ki} = \left\{\hat{g}^m_{ki} + \delta^m_{ki} : |\delta^m_{ki}| \le \delta^m_{ki,\max}, \forall k, i, m\right\}. \tag{10}$$

Similarly, the interference gains g^m_{nk} and g^m_{jk} can be expressed as

$$g^m_{nk} \in \mathcal{G}^m_{nk} = \left\{\hat{g}^m_{nk} + \delta^m_{nk} : |\delta^m_{nk}| \le \delta^m_{nk,\max}, \forall n, k, m\right\}, \tag{11}$$

$$g^m_{jk} \in \mathcal{G}^m_{jk} = \left\{\hat{g}^m_{jk} + \delta^m_{jk} : \left|\delta^m_{jk}\right| \le \delta^m_{jk,\max}, \forall k, j, m\right\}. \tag{12}$$

Taking into account the uncertainties of interference channel gains, problem (5) turns into the uncertain MOO problem:

$$\begin{aligned} &\min_{\boldsymbol{\rho},\mathbf{p}^{\mathrm{C}},\mathbf{p}^{\mathrm{D}}} \ \mathrm{f}_1\left(\boldsymbol{\rho}, \mathbf{p}^{\mathrm{C}}, \mathbf{p}^{\mathrm{D}}, \mathbf{g}^{\mathrm{C2B}}, \mathbf{g}^{\mathrm{D2B}}\right), \\ &\min_{\boldsymbol{\rho},\mathbf{p}^{\mathrm{C}},\mathbf{p}^{\mathrm{D}}} \ \mathrm{f}_2\left(\boldsymbol{\rho}, \mathbf{p}^{\mathrm{C}}, \mathbf{p}^{\mathrm{D}}\right), \\ &\text{s.t. } \mathrm{C1} - \mathrm{C7}, (9), (10), (11), (12). \end{aligned} \tag{13}$$

Defining $\mathcal{G} = \mathcal{G}^m_{n'i} \times \mathcal{G}^m_{ki} \times \mathcal{G}^m_{nk} \times \mathcal{G}^m_{kk'}$, we call $\left(\mathbf{g}^{\mathrm{C2B}}, \mathbf{g}^{\mathrm{D2B}}, \mathbf{g}^{\mathrm{C2D}}, \mathbf{g}^{\mathrm{D2D}}\right)$ is a scenario and problem (13) is an instance of the uncertain MOO problem $\mathcal{P}(\mathcal{G})$. In other words, problem $\mathcal{P}(\mathcal{G})$ is in fact a family of optimization problems with different scenarios $\left(\mathbf{g}^{\mathrm{C2B}}, \mathbf{g}^{\mathrm{D2B}}, \mathbf{g}^{\mathrm{C2D}}, \mathbf{g}^{\mathrm{D2D}}\right)$.

In this paper, we concentrate on *min-max robustness* [34], i.e., strict robustness, whose goal is to optimize the worst-case scenario of $\mathcal{P}(\mathcal{G})$ over all feasible solutions. Different from the existing literature [27]–[29] which study uncertain SOO problems, the uncertain problem $\mathcal{P}(\mathcal{G})$ considered in this paper is an uncertain MOO problem. Under this circumstance, we cannot evaluate solutions by just taking the worst case over all scenarios since there is a two-element vector of objective values for each scenario. Recalling the definition of *Pareto optimality* for a nominal MOO problem, we introduce the definition of *robust Pareto optimality*, i.e., robust efficiency [35] for an uncertain MOO problem as follows.

Definition 2 (Robust Pareto Optimality): Given an uncertain MOO problem with the uncertain parameter vector $\boldsymbol{\xi}$,

$$\begin{aligned} &\min_{\mathbf{x}} \ \mathrm{F}(\mathbf{x}, \boldsymbol{\xi}) = \left[\mathrm{f}_1(\mathbf{x}, \boldsymbol{\xi})\, \mathrm{f}_2(\mathbf{x}, \boldsymbol{\xi}) \cdots \mathrm{f}_O(\mathbf{x}, \boldsymbol{\xi})\right]^{\mathrm{T}}, \\ &\text{s.t. } \mathbf{x} \in \mathcal{X}, \quad \boldsymbol{\xi} \in \mathcal{U}, \end{aligned} \tag{14}$$

$\overline{\mathbf{x}} \in \mathcal{X}$ is robust Pareto optimal for problem (14) iff there does not exist $\mathbf{x} \in \mathcal{X} - \{\bar{\mathbf{x}}\}$ such that $\mathrm{F}_{\mathcal{U}}(\mathbf{x}) \subseteq \mathrm{F}_{\mathcal{U}}(\overline{\mathbf{x}}) - \mathbb{R}^O_{\ge}$ where $\mathrm{F}_{\mathcal{U}}(\mathbf{x}) = \{\mathrm{F}(\mathbf{x}, \boldsymbol{\xi}), \boldsymbol{\xi} \in \mathcal{U}\}$.

C. Robust Pareto Frontier

It can be observed from problem (13) that the second objective is deterministic, which implies that the uncertainty of the first objective is independent with the second one. Therefore, the existence of the worst case for the first objective indicates that the worst-case scenario exists for the uncertain MOO problem (13), which can be expressed as

$$\begin{aligned} &\max_{\mathbf{g}^{\mathrm{C2B}},\mathbf{g}^{\mathrm{D2B}}} \begin{bmatrix} \mathrm{f}_1\left(\boldsymbol{\rho}, \mathbf{p}^{\mathrm{C}}, \mathbf{p}^{\mathrm{D}}, \mathbf{g}^{\mathrm{C2B}}, \mathbf{g}^{\mathrm{D2B}}\right) \\ \mathrm{f}_2\left(\boldsymbol{\rho}, \mathbf{p}^{\mathrm{C}}, \mathbf{p}^{\mathrm{D}}\right) \end{bmatrix} \\ &\quad = \begin{bmatrix} \max_{\mathbf{g}^{\mathrm{C2B}},\mathbf{g}^{\mathrm{D2B}}} \mathrm{f}_1\left(\boldsymbol{\rho}, \mathbf{p}^{\mathrm{C}}, \mathbf{p}^{\mathrm{D}}, \mathbf{g}^{\mathrm{C2B}}, \mathbf{g}^{\mathrm{D2B}}\right) \\ \mathrm{f}_2\left(\boldsymbol{\rho}, \mathbf{p}^{\mathrm{C}}, \mathbf{p}^{\mathrm{D}}\right) \end{bmatrix} \end{aligned} \tag{15}$$

Furthermore, according to the definition of max-min robustness, the robust solutions of problem (13) should always satisfy all constraints for the given uncertainty region. Therefore, the robust counterpart of problem $\mathcal{P}(\mathcal{G})$ is readily obtained as

$$\begin{aligned} &\min_{\boldsymbol{\rho},\mathbf{p}^{\mathrm{C}},\mathbf{p}^{\mathrm{D}}} \ \max_{\mathbf{g}^{\mathrm{C2B}},\mathbf{g}^{\mathrm{D2B}}} \mathrm{f}_1\left(\boldsymbol{\rho}, \mathbf{p}^{\mathrm{C}}, \mathbf{p}^{\mathrm{D}}, \mathbf{g}^{\mathrm{C2B}}, \mathbf{g}^{\mathrm{D2B}}\right), \\ &\min_{\boldsymbol{\rho},\mathbf{p}^{\mathrm{C}},\mathbf{p}^{\mathrm{D}}} \ \mathrm{f}_2\left(\boldsymbol{\rho}, \mathbf{p}^{\mathrm{C}}, \mathbf{p}^{\mathrm{D}}\right), \\ &\text{s.t. } \mathrm{C1} - \mathrm{C5}, \\ &\quad \mathrm{C6}': \min_{\mathbf{g}^{\mathrm{C2B}},\mathbf{g}^{\mathrm{D2B}}} R^{\mathrm{C}}_n \ge R^{\mathrm{C}}_{n,\min}, \quad \forall n \in \mathcal{C}, \\ &\quad \mathrm{C7}': \min_{\mathbf{g}^{\mathrm{C2D}},\mathbf{g}^{\mathrm{D2D}}} R^{\mathrm{D}}_k \ge R^{\mathrm{D}}_{k,\min}, \quad \forall k \in \mathcal{D}, \end{aligned} \tag{16}$$

and the following theorem further clarifies the relationship between problem $\mathcal{P}(\mathcal{G})$ and its robust counterpart (16).

Theorem 1: If $\max_{\mathbf{g}^{\mathrm{C2B}},\mathbf{g}^{\mathrm{D2B}}} \mathrm{f}_1(\boldsymbol{\rho},\ \mathbf{p}^{\mathrm{C}},\ \mathbf{p}^{\mathrm{D}},\ \mathbf{g}^{\mathrm{C2B}},\ \mathbf{g}^{\mathrm{D2B}})$, $\min_{\mathbf{g}^{\mathrm{C2B}},\mathbf{g}^{\mathrm{D2B}}} R_n^{\mathrm{C}}$, and $\min_{\mathbf{g}^{\mathrm{C2D}},\mathbf{g}^{\mathrm{D2D}}} R_k^{\mathrm{D}}$ exist for all $\left(\boldsymbol{\rho},\mathbf{p}^{\mathrm{C}},\mathbf{p}^{\mathrm{D}}\right)$, we have that $\left(\boldsymbol{\rho}^*,\mathbf{p}^{\mathrm{C}*},\mathbf{p}^{\mathrm{D}*}\right)$ is Pareto optimal for problem (16) iff $\left(\boldsymbol{\rho}^*,\mathbf{p}^{\mathrm{C}*},\mathbf{p}^{\mathrm{D}*}\right)$ is robust Pareto optimal for problem $\mathcal{P}(\mathcal{G})$.

Proof: See Appendix A. ■

According to Theorem 1, to find all the robust Pareto optimal solutions of $\mathcal{P}(\mathcal{G})$, we can alternatively find all Pareto optimal solutions of problem (16). Thus, in this paper, ε-constraint method is employed to transform problem (16) into a SOO problem, which is guaranteed to find all Pareto optimal solutions even for non-convex problems [33]. By minimizing one objective and converting the other objective into a constraint with an adjustable upper bound, we can transform problem (16) into

$$\begin{aligned}&\min_{\boldsymbol{\rho},\mathbf{p}^{\mathrm{C}},\ \mathbf{p}^{\mathrm{D}}}\ \max_{\mathbf{g}^{\mathrm{C2B}},\mathbf{g}^{\mathrm{D2B}}} \mathrm{f}_1\left(\boldsymbol{\rho},\mathbf{p}^{\mathrm{C}},\mathbf{p}^{\mathrm{D}},\mathbf{g}^{\mathrm{C2B}},\mathbf{g}^{\mathrm{D2B}}\right),\\ &\text{s.t. } \mathrm{C1}-\mathrm{C5},\mathrm{C6}',\mathrm{C7}',\\ &\qquad \mathrm{C8}:\mathrm{f}_2\left(\boldsymbol{\rho},\mathbf{p}^{\mathrm{C}},\mathbf{p}^{\mathrm{D}}\right)\le\varepsilon,\end{aligned} \tag{17}$$

where ε can be adjusted to achieve different kinds of tradeoff between EE and SE.

Theorem 2: If $\max_{\mathbf{g}^{\mathrm{C2B}},\mathbf{g}^{\mathrm{D2B}}} \mathrm{f}_1(\boldsymbol{\rho},\ \mathbf{p}^{\mathrm{C}},\ \mathbf{p}^{\mathrm{D}},\ \mathbf{g}^{\mathrm{C2B}},\ \mathbf{g}^{\mathrm{D2B}})$, $\min_{\mathbf{g}^{\mathrm{C2B}},\mathbf{g}^{\mathrm{D2B}}} R_n^{\mathrm{C}}$, and $\min_{\mathbf{g}^{\mathrm{C2D}},\mathbf{g}^{\mathrm{D2D}}} R_k^{\mathrm{D}}$ exist for all $\left(\boldsymbol{\rho},\mathbf{p}^{\mathrm{C}},\mathbf{p}^{\mathrm{D}}\right)$, $\left(\boldsymbol{\rho}^*,\mathbf{p}^{\mathrm{C}*},\mathbf{p}^{\mathrm{D}*}\right)$ is robust Pareto optimal for problem $\mathcal{P}(\mathcal{G})$ iff there exists ε such that $\left(\boldsymbol{\rho}^*,\mathbf{p}^{\mathrm{C}*},\mathbf{p}^{\mathrm{D}*}\right)$ is the unique optimal solution to problem (17).

Proof: See Appendix B. ■

Remark 3: From Theorem 2, it can be concluded that the ε-constraint method is guaranteed to find all robust Pareto optimal solutions of problem $\mathcal{P}(\mathcal{G})$. In other words, the proposed framework for robust multi-objective optimization can provide an entire *robust Pareto frontier* for the uncertain MOO problem $\mathcal{P}(\mathcal{G})$, just like the complete Pareto optimal set for a nominal MOO problem. Note that this framework is general enough to be applied to other systems with interference channel uncertainties.

D. Closed-Form Expression

To facilitate further processing, we need to derive the closed-form expression of problem (17). First of all, to address the uncertainty shown in the objective, the following results can be found:

$$\begin{aligned}g_{n'i}^{m*}&=\arg\max_{g_{n'i}^m\in\mathcal{G}_{n'i}^m}\mathrm{f}_1\left(\boldsymbol{\rho},\mathbf{p}^{\mathrm{C}},\mathbf{p}^{\mathrm{D}},\mathbf{g}^{\mathrm{C2B}},\mathbf{g}^{\mathrm{D2B}}\right)\\&=\arg\min_{g_{n'i}^m\in\mathcal{G}_{n'i}^m}\sum_{n\in\mathcal{C}}R_n^{\mathrm{C}}\\&=\arg\min_{g_{n'i}^m\in\left\{\hat{g}_{n'i}^m+\delta_{n'i}^m:\left|\delta_{n'i}^m\right|\le\delta_{n'i,\max}^m\right\}}r_{n^*m}^{\mathrm{C}}\\&=\hat{g}_{n'i}^m+\delta_{n'i,\max}^m,\end{aligned} \tag{18}$$

where

$$r_{n^*m}^{\mathrm{C}}=\log_2\left(1+\frac{p_{n^*m}^{\mathrm{C}}h_{n^*i}^m}{I_{n^*m}^{\mathrm{C}}+\sigma^2}\right), \tag{19}$$

and n^* denotes the index of the CU which is associated with the *i*-BS and occupies the *m*-th RB. Similarly, it can be obtained that

$$g_{ki}^{m*}=\arg\max_{g_{ki}^m\in\mathcal{G}_{ki}^m}\mathrm{f}_1\left(\boldsymbol{\rho},\mathbf{p}^{\mathrm{C}},\mathbf{p}^{\mathrm{D}},\mathbf{g}^{\mathrm{C2B}},\mathbf{g}^{\mathrm{D2B}}\right)=\hat{g}_{ki}^m+\delta_{ki,\max}^m. \tag{20}$$

Then, the constraints C6′ and C7′ can be re-expressed as

$$\mathrm{C6}':\ \sum_{m\in\mathcal{M}_n^{\mathrm{C}}}\log_2\left(1+\frac{p_{nm}^{\mathrm{C}}h_{ni}^m}{I_{nm}^{\mathrm{C}*}+\sigma^2}\right)\ge R_{n,\min}^{\mathrm{C}},\quad\forall n\in\mathcal{C}, \tag{21a}$$

$$\mathrm{C7}':\ \sum_{m\in\mathcal{M}}\rho_{km}\log_2\left(1+\frac{p_k^{\mathrm{D}}h_k^m}{I_{km}^{\mathrm{D}*}+\sigma^2}\right)\ge R_{k,\min}^{\mathrm{D}},\quad\forall k\in\mathcal{D}, \tag{21b}$$

where $I_{nm}^{\mathrm{C}*}=\sum_{n'\in\mathcal{C}_m,n'\ne n}p_{n'm}^{\mathrm{C}}g_{n'i}^{m*}+\sum_{k\in\mathcal{D}}\rho_{km}p_k^{\mathrm{D}}g_{ki}^{m*}$, $I_{km}^{\mathrm{D}*}=\sum_{n\in\mathcal{C}_m}p_{nm}^{\mathrm{C}}g_{nk}^{m*}+\sum_{j\ne k,j\in\mathcal{D}}\rho_{jm}p_j^{\mathrm{D}}g_{jk}^{m*}$, $g_{nk}^{m*}=\hat{g}_{nk}^m+\delta_{nk,\max}^m$, and $g_{jk}^{m*}=\hat{g}_{jk}^m+\delta_{jk,\max}^m$. Thus, the closed-form expression of problem (17) can be expressed as

$$\begin{aligned}&\min_{\boldsymbol{\rho},\mathbf{p}^{\mathrm{C}},\mathbf{p}^{\mathrm{D}}}\ \mathrm{f}_1\left(\boldsymbol{\rho},\mathbf{p}^{\mathrm{C}},\mathbf{p}^{\mathrm{D}},\mathbf{g}^{\mathrm{C2B}*},\mathbf{g}^{\mathrm{D2B}*}\right),\\&\text{s.t. } \mathrm{C1}-\mathrm{C5},\mathrm{C6}',\mathrm{C7}',\mathrm{C8}.\end{aligned} \tag{22}$$

IV. Joint Spectrum Allocation and Power Coordination

The transformed problem (22) factors the tradeoff between the system EE and SE for CUs as well as strict QoS requirements of all D2D pairs and CUs. However, this problem is highly non-convex because of the integer variable ρ_{km} and mutual interference not only among CUs and D2D pairs but also among D2D pairs sharing the same RB, which is NP-hard to find the global optimal RB allocation and power coordination solution. Therefore, in this section, we aim at finding a practical algorithm for the joint optimization of spectrum allocation and power coordination. With the employment of primal decomposition [36], the original problem can be divided into two subproblems, and a two-stage iterative algorithm is developed which optimizes the RB allocation and power coordination in turn. With the given RB allocation variable $\boldsymbol{\rho}=\boldsymbol{\rho}'$ in problem (22), the *joint power coordination of CUs and D2D pairs problem* can be obtained as

$$\begin{aligned}&\max_{\mathbf{p}^{\mathrm{C}},\mathbf{p}^{\mathrm{D}}}\ R_{\mathrm{tot}}\left(\mathbf{p}^{\mathrm{C}},\mathbf{p}^{\mathrm{D}}\right)=\sum_{n\in\mathcal{C}}R_n^{\mathrm{C}}\left(\boldsymbol{\rho}',\mathbf{p}^{\mathrm{C}},\mathbf{p}^{\mathrm{D}},\mathbf{g}^{\mathrm{C2B}*},\mathbf{g}^{\mathrm{D2B}*}\right),\\&\text{s.t. } \mathrm{C4},\mathrm{C5},\mathrm{C6}',\mathrm{C7}',\mathrm{C8}.\end{aligned} \tag{23}$$

Contrarily, by fixing $\mathbf{p}^{\mathrm{C}}=\mathbf{p}^{\mathrm{C}'}$ and $\mathbf{p}^{\mathrm{D}}=\mathbf{p}^{\mathrm{D}'}$ in problem (22), the *RB allocation problem* can be presented as

$$\begin{aligned}&\min_{\boldsymbol{\rho}}\ R_{\mathrm{tot}}\left(\boldsymbol{\rho}\right)=\sum_{n\in\mathcal{C}}R_n^{\mathrm{C}}\left(\boldsymbol{\rho},\mathbf{p}^{\mathrm{C}'},\mathbf{p}^{\mathrm{D}'},\mathbf{g}^{\mathrm{C2B}*},\mathbf{g}^{\mathrm{D2B}*}\right),\\&\text{s.t. } \mathrm{C1}-\mathrm{C3},\mathrm{C6}',\mathrm{C7}'.\end{aligned} \tag{24}$$

Note that we have removed constant items in (23) and (24) for the purpose of simplicity.

A. Joint Power Coordination of CUs and D2D Pairs

As mentioned above, the power coordination problem is non-convex because of existing mutual interference. To address this problem, we first re-express the rate function of CU-*n* as

$$R_n^{\mathrm{C}}\left(\mathbf{p}^{\mathrm{C}},\mathbf{p}^{\mathrm{D}}\right)=X_n\left(\mathbf{p}^{\mathrm{C}},\mathbf{p}^{\mathrm{D}}\right)-Y_n\left(\mathbf{p}^{\mathrm{C}},\mathbf{p}^{\mathrm{D}}\right) \tag{25}$$

where both functions $X_n\left(\mathbf{p}^{\mathrm{C}},\mathbf{p}^{\mathrm{D}}\right)$ and $Y_n\left(\mathbf{p}^{\mathrm{C}},\mathbf{p}^{\mathrm{D}}\right)$ are concave and defined as

$$X_n\left(\mathbf{p}^{\mathrm{C}},\mathbf{p}^{\mathrm{D}}\right)=\sum_{m\in\mathcal{M}_n^{\mathrm{C}}}\log_2\left(p_{nm}^{\mathrm{C}}h_{ni}^{m}+I_{nm}^{\mathrm{C}*}+\sigma^2\right), \tag{26a}$$

$$Y_n\left(\mathbf{p}^{\mathrm{C}},\mathbf{p}^{\mathrm{D}}\right)=\sum_{m\in\mathcal{M}_n^{\mathrm{C}}}\log_2\left(I_{nm}^{\mathrm{C}*}+\sigma^2\right). \tag{26b}$$

Thus, the objective of problem (23) is actually the difference of two concave functions:

$$R_{\mathrm{tot}}\left(\mathbf{p}^{\mathrm{C}},\mathbf{p}^{\mathrm{D}}\right)=\sum_{n\in\mathcal{C}}X_n\left(\mathbf{p}^{\mathrm{C}},\mathbf{p}^{\mathrm{D}}\right)-\sum_{n\in\mathcal{C}}Y_n\left(\mathbf{p}^{\mathrm{C}},\mathbf{p}^{\mathrm{D}}\right). \tag{27}$$

To find the power coordination solution within affordable computational complexity, sequential optimization [37] is adopt in this paper, which can generate a series of improved feasible solutions [15], [25]. Specifically, for a given initial point $\left(\mathbf{p}^{\mathrm{C},(0)},\mathbf{p}^{\mathrm{D},(0)}\right)$, at the *t*-th iteration, the objective of problem (23) can be approximated as

$$\tilde{R}_{\mathrm{tot}}^{(t)}\left(\mathbf{p}^{\mathrm{C}},\mathbf{p}^{\mathrm{D}}\right)=\sum_{n\in\mathcal{C}}X_n\left(\mathbf{p}^{\mathrm{C}},\mathbf{p}^{\mathrm{D}}\right)-\sum_{n\in\mathcal{C}}\tilde{Y}_n^{(t)}\left(\mathbf{p}^{\mathrm{C}},\mathbf{p}^{\mathrm{D}}\right), \tag{28}$$

where $Y_n\left(\mathbf{p}^{\mathrm{C}},\mathbf{p}^{\mathrm{D}}\right)$ is approximated as

$$\begin{aligned}
&Y_n\left(\mathbf{p}^{\mathrm{C}},\mathbf{p}^{\mathrm{D}}\right)\le\tilde{Y}_n^{(t)}\left(\mathbf{p}^{\mathrm{C}},\mathbf{p}^{\mathrm{D}}\right)\\
&=Y_n\left(\mathbf{p}^{\mathrm{C},(t-1)},\mathbf{p}^{\mathrm{D},(t-1)}\right)\\
&+\sum_{n\in\mathcal{C}}\sum_{m\in\mathcal{M}_n^{\mathrm{C}}}\left(p_{nm}^{\mathrm{C}}-p_{nm}^{\mathrm{C},(t-1)}\right)\left.\frac{\partial Y_n\left(\mathbf{p}^{\mathrm{C}},\mathbf{p}^{\mathrm{D}}\right)}{\partial p_{nm}^{\mathrm{C}}}\right|_{\substack{\mathbf{p}^{\mathrm{C}}=\mathbf{p}^{\mathrm{C},(t-1)},\\ \mathbf{p}^{\mathrm{D}}=\mathbf{p}^{\mathrm{D},(t-1)}}}\\
&+\sum_{k\in\mathcal{D}}\left(p_k^{\mathrm{D}}-p_k^{\mathrm{D},(t-1)}\right)\left.\frac{\partial Y_n\left(\mathbf{p}^{\mathrm{C}},\mathbf{p}^{\mathrm{D}}\right)}{\partial p_k^{\mathrm{D}}}\right|_{\substack{\mathbf{p}^{\mathrm{C}}=\mathbf{p}^{\mathrm{C},(t-1)},\\ \mathbf{p}^{\mathrm{D}}=\mathbf{p}^{\mathrm{D},(t-1)}}}
\end{aligned} \tag{29}$$

Note that the equality of (29) holds when $\left(\mathbf{p}^{\mathrm{C}},\mathbf{p}^{\mathrm{D}}\right)=\left(\mathbf{p}^{\mathrm{C},(t-1)},\mathbf{p}^{\mathrm{D},(t-1)}\right)$. In the same way, the constraint C6′ is near

$$\mathrm{C6}'':X_n\left(\mathbf{p}^{\mathrm{C}},\mathbf{p}^{\mathrm{D}}\right)-\tilde{Y}_n^{(t)}\left(\mathbf{p}^{\mathrm{C}},\mathbf{p}^{\mathrm{D}}\right)\ge R_{n,\min}^{\mathrm{C}},\quad\forall n. \tag{30}$$

In addition, the constraint C7′ is actually a linear constraint, which can be equivalently transformed into

$$\mathrm{C7}'':p_k^{\mathrm{D}}h_k^{\hat{m}(k)}-\left(2^{R_{k,\min}^{\mathrm{D}}}-1\right)\left(I_{k\hat{m}(k)}^{\mathrm{D}*}+\sigma^2\right)\ge 0,\quad\forall k, \tag{31}$$

where $\hat{m}(k)$ denotes the index of RB allocated to the *k*-th D2D pair, i.e., $\rho'_{k\hat{m}(k)}=1$. Consequently, at the *t*-th iteration, $\left(\mathbf{p}^{\mathrm{C},(t)},\mathbf{p}^{\mathrm{D},(t)}\right)$ can be obtained by finding the optimum of the convex problem

$$\begin{aligned}
&\max_{\mathbf{p}^{\mathrm{C}},\mathbf{p}^{\mathrm{D}}}\ \tilde{R}_{\mathrm{tot}}^{(t)}\left(\mathbf{p}^{\mathrm{C}},\mathbf{p}^{\mathrm{D}}\right),\\
&\text{s.t. C4, C5, C6}'',\text{C7}'',\text{C8},
\end{aligned} \tag{32}$$

which is readily solved via standard algorithms with polynomial complexity [38].

To tighten the approximation in (29) and generate the near-optimal solution of (23), it is essential to iteratively set new power coordination solution $\left(\mathbf{p}^{\mathrm{C},(t)},\mathbf{p}^{\mathrm{D},(t)}\right)$ and solve problem (32) until convergence. The above steps are summarized in **Algorithm 1**, and its effectiveness and convergence are proved as follows.

Algorithm 1 D. C. Programming Algorithm for Joint Power Coordination

1. Initialize $t=0$, $flag_{\mathrm{pc}}=1$, $\phi=0.01$, and find an initial feasible solution $\left(\mathbf{p}^{\mathrm{C},(0)},\mathbf{p}^{\mathrm{D},(0)}\right)$.
2. **while** $flag_{\mathrm{pc}}>\phi$, **do**
3. $t=t+1$;
4. Calculate $\tilde{Y}_n^{(t)}\left(\mathbf{p}^{\mathrm{C}},\mathbf{p}^{\mathrm{D}}\right)$ with $\left(\mathbf{p}^{\mathrm{C},(t-1)},\mathbf{p}^{\mathrm{D},(t-1)}\right)$;
5. Solve problem (32) and obtain $\left(\mathbf{p}^{\mathrm{C}(t)},\mathbf{p}^{\mathrm{D},(t)}\right)$;
6. Calculate $\Delta p_{nm}^{\mathrm{C},(t)}=\left|\frac{p_{nm}^{\mathrm{C},(t)}-p_{nm}^{\mathrm{C},(t-1)}}{p_{nm}^{\mathrm{C},(t-1)}}\right|,\forall n,m$;
7. Calculate $\Delta p_k^{\mathrm{D},(t)}=\left|\frac{p_k^{\mathrm{D},(t)}-p_k^{\mathrm{D},(t-1)}}{p_k^{\mathrm{D},(t-1)}}\right|,\forall k$;
8. Calculate $flag_{\mathrm{pc}}=\max_{n,m,k}\left\{\Delta p_{nm}^{\mathrm{C},(t)},\Delta p_k^{\mathrm{D},(t)}\right\}$.
9. **end while**

Theorem 3: Algorithm 1 monotonically increases the value of $R_{\mathrm{tot}}\left(\mathbf{p}^{\mathrm{C}},\mathbf{p}^{\mathrm{D}}\right)$ with the number of iterations and finally converges to the point satisfying the KKT conditions of problem (23).

Proof: See Appendix C. ■

Note that for the given threshold $\phi>0$, the iterative process of Algorithm 1 terminates after finite iterations at either $flag_{\mathrm{pc}}<\phi$ or $\left|\frac{R_{\mathrm{tot}}\left(\mathbf{p}^{\mathrm{C},(t)},\mathbf{p}^{\mathrm{D},(t)}\right)-R_{\mathrm{tot}}\left(\mathbf{p}^{\mathrm{C},(t-1)},\mathbf{p}^{\mathrm{D},(t-1)}\right)}{R_{\mathrm{tot}}\left(\mathbf{p}^{\mathrm{C},(t-1)},\mathbf{p}^{\mathrm{D},(t-1)}\right)}\right|<\phi$.

B. Resource Block Allocation

To solve problem (24), we introduce a two-sided matching game defined as below, where RBs and D2D pairs are two opposite sets of agents which aim at maximizing their own utilities.

Definition 3: The matching game between RBs and D2D pairs is expressed as a function M which maps the set of $\mathcal{M}\cup\mathcal{D}$ to the set of $\mathcal{M}\cup\mathcal{D}$ such that for the *m*-th RB $RB_m\in\mathcal{M}$ and the *k*-th D2D pair $DP_k\in\mathcal{D}$:
(a) $\mathrm{M}\left(RB_m\right)\subseteq\mathcal{D}$;
(b) $\mathrm{M}\left(DP_k\right)\in\mathcal{M}$;
(c) $\left|\mathrm{M}\left(RB_m\right)\right|\le Q$;
(d) $\left|\mathrm{M}\left(DP_k\right)\right|\le 1$;
(e) $DP_k\in\mathrm{M}\left(RB_m\right)\Leftrightarrow RB_m=\mathrm{M}\left(DP_k\right)$.
Condition (a) and (c) indicate that each RB is matched with at most Q D2D pairs, while condition (b) and (d) represent that each D2D pair can only match with one RB.

Condition (e) implies that CUs and D2D pairs are matched mutually. Besides, $\mathrm{M}(RB_m)$ or $\mathrm{M}(DP_k)$ can be the empty set if no D2D pairs or RBs can be matched with the *m*-th RB or the *k*-th D2D pair.

Then, to measure the motivation of each agent, we first define the **utility of the *m*-th RB** as the transmission data rate of all CUs on it, i.e.,

$$U_{RB_m}(\mathrm{M}) = \sum_{n \in \mathcal{C}_m} R_{nm}^{\mathrm{C}}(\mathrm{M}), \quad \forall m \in \mathcal{M}, \tag{33}$$

and similarly, the **utility of the *k*-th D2D pair** can be expressed as

$$U_{DP_k}(\mathrm{M}) = R_k^{\mathrm{D}}(\mathrm{M}), \quad \forall k \in \mathcal{D}. \tag{34}$$

With the above definitions, all CUs and D2D pairs can construct their preference lists with the descending order of utilities.

Remark 4: Different from the conventional model of the two-sided matching where preference lists are fixed during the matching process, the matching described above is a *matching with externalities*, where preference lists will change as the matching game proceeds due to the mutual interference among CUs and D2D pairs sharing the same RB. For instance, if the *k*-th D2D pair is matched with RB-*m*, the interference on the *m*-th RB will increase, and thus other D2D pairs may change their preferences since the utility functions vary with interference. In this case, the preference list of each D2D pair depends on the choices of other agents. Consequently, the matching game considered in this paper is more complicated compared to the traditional case.

To better illustrate the interdependency of agents' preference lists, we introduce the definitions of *swap matching* and *swap-blocking pair* in the following.

Definition 4: For a given matching M where $\mathrm{M}(DP_k) = RB_m$, and $\mathrm{M}(DP_j) = RB_l$, the swap matching is defined as $\mathrm{M}_{jl}^{km} = \mathrm{M} \backslash \{(DP_k, RB_m), (DP_j, RB_l)\} \cup \{(DP_k, RB_l), (DP_j, RB_m)\}$, which denotes that the two specific D2D pairs exchange their matched RBs while the other D2D pairs remain unchanged. Besides, the swap matching M_{jl}^{km} will be approved only if

1) $\forall a \in \{DP_k, DP_j, RB_m, RB_l\}$, $U_a\left(\mathrm{M}_{jl}^{km}\right) \geq U_a(\mathrm{M})$;

2) $\exists a \in \{DP_k, DP_j, RB_m, RB_l\}$, $U_a\left(\mathrm{M}_{jl}^{km}\right) > U_a(\mathrm{M})$,

and (DP_k, DP_j) is called a swap-blocking pair in M.
Note that the above definition indicates that only if the utilities of all involved players are not reduced and at least one player's utility increases, a swap matching will be approved.

Now, we first propose a low-complexity algorithm as an initial base line, which is summarized in **Algorithm 2**. First of all, each D2D pair proposes to its most preferred RB, which is ranked first in its preference list. After receiving the proposal, each RB will reject its least-preferred D2D pair in its waiting list repeatedly until the minimum rate requirements of all CUs are satisfied and at most *Q* D2D pairs are accepted. The above steps will be carried out until all D2D pairs have been matched.

Furthermore, from Definition 4, it can be observed that swap operations can help to improve the utilities of agents and therefore the performance of the spectrum allocation algorithm. Inspired by this observation, the further swap matching algorithm is developed and summarized in **Algorithm 3**. At the beginning, each D2D pair will search another D2D pair or available vacancies in other RBs to check if they can form a swap-blocking pair. If the swap matching is approved, the matching will update to the swap matching. The above process will continue until there does not exist any swap-blocking pairs.

For the aforementioned matching game with externalities, the traditional definition for the stability of a matching game is not guaranteed. Instead, we concentrate on finding the *two-sided exchange-stable matching* [39] in this paper, which is defined as below.

Algorithm 2 Initial Matching Algorithm for Spectrum Allocation

1. **for** each D2D pair $DP_k \in \mathcal{D}$
2. Calculate $R_k^{\mathrm{D}}\big|_{\mathrm{M}(DP_k)=RB_m}$, $\forall RB_m \in \mathcal{M}$;
3. Establish the preference list $\mathcal{P}_k^{\mathrm{D}}$ by sorting RB_m in descending order of $R_k^{\mathrm{D}}\big|_{\mathrm{M}(DP_k)=RB_m}$;
4. **end for**
5. Initialize the set of the unmatched D2D pairs $\mathcal{D}_{\mathrm{u}} = \mathcal{D}$;
6. **while** $\mathcal{D}_{\mathrm{u}} \neq \phi$
7. **for** each D2D pair $DP_k \in \mathcal{D}_{\mathrm{u}}$
8. DP_k sends a request to its most-preferred RB in $\mathcal{P}_k^{\mathrm{D}}$, e.g., RB_m, by setting $\rho_{km}^{\mathrm{I}} = 1$;
9. **end For**
10. **for** each RB $RB_m \in \mathcal{M}$
11. Establish waiting list $\mathcal{W}_m^{\mathrm{RB}} = \left\{DP_k \left| \rho_{km}^{\mathrm{I}} = 1 \right.\right\}$;
12. Remove $\mathcal{W}_m^{\mathrm{RB}}$ from $\mathcal{D}_{\mathrm{u}}$;
13. **while** the minimum rate requirements of CUs are not satisfied or $\left|\mathcal{W}_m^{\mathrm{RB}}\right| > Q$
14. Find the least-preferred D2D pair in $\mathcal{W}_m^{\mathrm{RB}}$, denoted as $DP_{k'}$;
15. Reject $DP_{k'}$ by setting $\rho_{k'm}^{\mathrm{I}} = 0$;
16. Add $DP_{k'}$ into $\mathcal{D}_{\mathrm{u}}$;
17. Remove RB_m from $\mathcal{P}_{k'}^{\mathrm{D}}$;
18. **end while**
19. **end for**
20. **end while**
21. **Output** the initial RB allocation solution $\boldsymbol{\rho}^{\mathrm{I}}$.

Algorithm 3 Further Swap Matching Algorithm for Spectrum Allocation

1. **Initialize** the spectrum allocation solution $\boldsymbol{\rho}^{\mathrm{I}}$.
2. **for** each D2D pair $DP_k \in \mathcal{D}$
3. DP_k searches DP_j or vacancies O_l on RB-*l*;
4. Check if (DP_k, DP_j) or (DP_k, O_l) is a swap-blocking pair;
5. If approved, DP_k exchanges its RB with DP_j or moves to the *l*-th RB;
6. Update the matching state;
7. Repeat 3-6 until all swap matchings checked.
8. **end for**
9. **Output** the convergent matching state $\boldsymbol{\rho}^*$.

Definition 5: A matching M is called a two-sided exchange-stable matching if no swap-blocking pair exists.

Then, we have the following theorem for Algorithm 3.

Theorem 4: Algorithm 3 is guaranteed to converge to a two-sided exchange-stable matching within a limited number of iterations.

Proof: See Appendix D. ■

C. Two-Stage Iterative Algorithm and Performance Analysis

Up to now, the solutions of subproblems (23) and (24) have been obtained via Algorithm 1, and Algorithm 2-3, respectively. Thus, the original SOO problem (22) can be readily solved by developing the two-stage iterative algorithm as organized in **Algorithm 4**, and the following theorem illustrates its *effectiveness* and *convergence*.

Algorithm 4 Two-Stage Iterative Algorithm for Joint Spectrum Allocation and Power Coordination

1. For any given tradeoff parameter ε,
2. Initialize $\tau = 0$, $flag = 1$, $\Phi = 0.01$;
3. Initialize $p_{nm}^{\mathrm{C}} = \frac{\varepsilon - Np_s}{\alpha N |\mathcal{M}_n^{\mathrm{C}}|}$, $p_k^{\mathrm{D}} = p_{\max}^{\mathrm{D}}$;
4. Initialize $\boldsymbol{\rho}^0$ via Algorithm 2;
5. **while** $flag > \Phi$, **do**
6. $\tau = \tau + 1$;
7. Calculate $\boldsymbol{\rho}^\tau$ via Algorithm 3;
8. Calculate $\left(\mathbf{p}^{\mathrm{C},(\tau)}, \mathbf{p}^{\mathrm{D},(\tau)}\right)$ via Algorithm 1 with $\boldsymbol{\rho}^\tau$;
9. Calculate $flag = \max\limits_{k,m} \left| \rho_{km}^{(\tau)} - \rho_{km}^{(\tau-1)} \right|$.
10. **end while**

Theorem 5: Algorithm 4 monotonically decreases the objective of problem (22) at each iteration, and finally converges in a finite amount of iterations for a given threshold Φ.

Proof: See Appendix E. ■

For the spectrum allocation problem, its computational complexity is mainly up to the swap matching algorithm, i.e., Algorithm 3. Since there are at most $\frac{1}{2}K(M-1)Q$ potential swap-blocking pairs, the computation complexity of Algorithm 3 approaches to $\mathcal{O}(K(M-1)Q)$. In addition, the power coordination problem is highly non-convex because of mutual interference among D2D pairs and CUs. It is rather difficult to find its global optimal solution, and thus Algorithm 1 is proposed to solve problem (23), which is guaranteed to find the local optimum. Specifically, as a standard convex problem is solved at each iteration, only polynomial computational complexity $\mathcal{O}\left((N+K)^{\mu}(NM+K)^{v}\right)$ is required via the interior point method [18], [20], where μ and v are positive constant. Besides, Algorithm 4 converges fast as verified by simulation results (see Fig. 3). In conclusion, the total computational complexity of Algorithm 4 for the joint optimization of spectrum allocation and power coordination is $\mathcal{O}\left(KQ(M-1)(N+K)^{\mu}(NM+K)^{\nu}\right)$. In other words, the proposed algorithm only requires polynomial complexity to solve problem (22).

TABLE I
SIMULATION PARAMETERS SETTING

Parameters	Value
Cell radius	500 m
Maximum distance of D2D pairs	50 m
Number of resource blocks	12
Amplifier's efficiency	0.38
Fixed power of CUs	1 W
Maximum transmit power of D2D pairs	0.1 W
Maximum transmit power of CUs	0.2 W
Minimum rate requirements of D2D pairs	1 bit/s/Hz
Minimum rate requirements of CUs	2 bit/s/Hz
Quota of each resource block	2
Number of CUs	6
Number of D2D pairs	8
Normalized error bound of interference channels	0.05

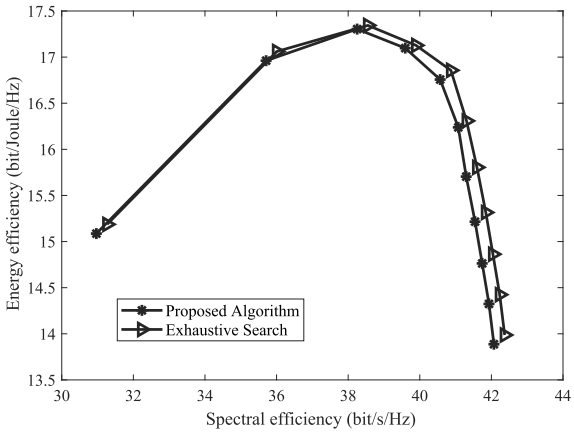

Fig. 2. Energy and spectral efficiency tradeoff for the proposed algorithm and the exhaustive search.

V. SIMULATION RESULTS

In this section, numerical results are presented to demonstrate the performance of our proposed algorithm. It is assumed that there are one macro BS in the cell center, three pico BSs located at the circle with the radius of 200m, and randomly distributed D2D pairs as well as CUs. The large-scale channel gain between two nodes is composed of path loss and shadow fading, where the path loss is modelled as $128.1 + 37.6\log_{10} d$ (km), and the standard derivation of shadow fading is 8 dB. Besides, it is assumed that all channels undergo Rayleigh fading, and the other related simulation parameters and their default values are shown in Table I. For notational brevity, we use $\delta_{\max}$ to represent the normalized error bound for all interference channel uncertainty regions, which is normalized by the corresponding estimate. Please note that if there are not particular statements, the parameter values mentioned in Table I are default values used to generate all the following results.

1) Optimality and Convergence of the Proposed Algorithm: We first compare the proposed two-stage iterative algorithm with the exhaustive search method to verify its optimality. As the exhaustive search method is achieved with exponential computational complexity, the small-scale case of $N = 2$, $K = 3$, $M = 4$ is presented as an instance in Fig. 2.

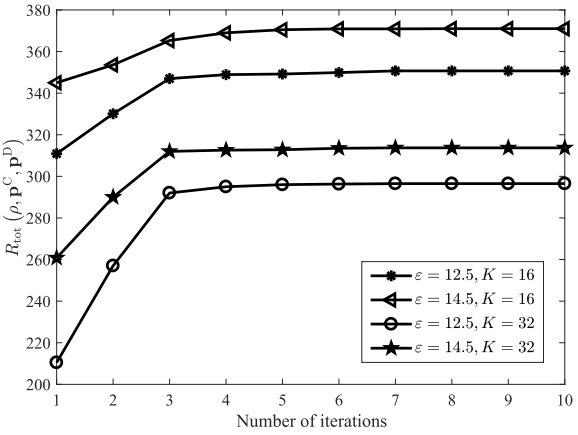

Fig. 3. The convergence procedure of Algorithm 4.

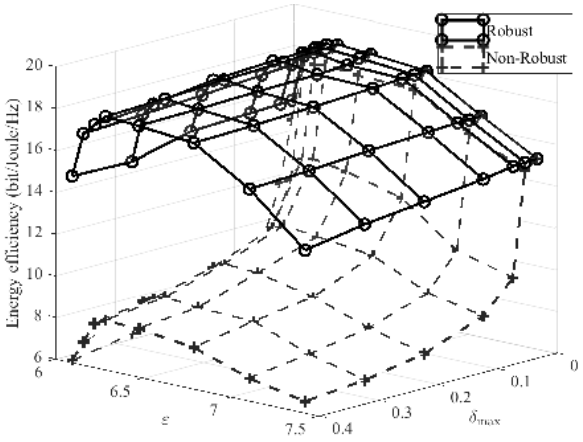

Fig. 4. The energy efficiency comparison under different ε and $\delta_{\max}$.

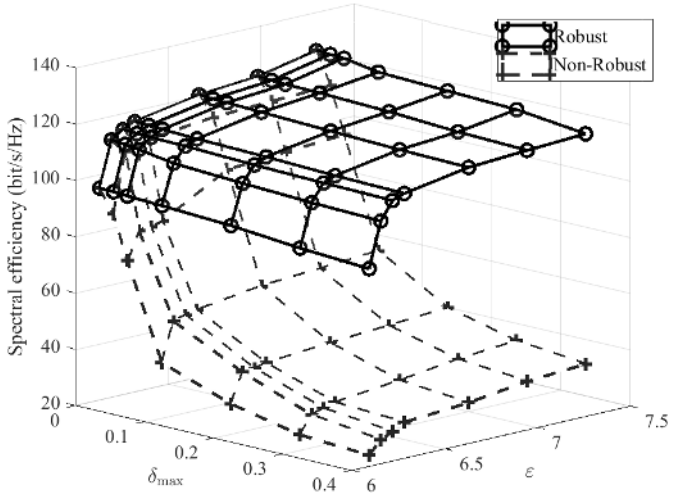

Fig. 5. The spectral efficiency comparison under different ε and $\delta_{\max}$.

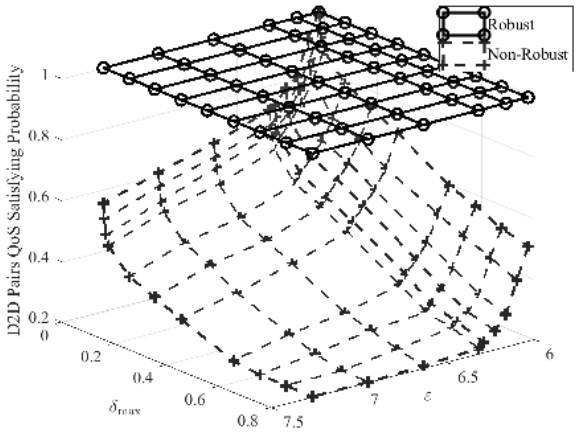

Fig. 6. The D2D pairs QoS satisfying probability under different ε and $\delta_{\max}$.

As shown in Fig. 2, our proposed algorithm approaches the exhaustive search algorithm in terms of the tradeoff between EE and SE. Then, we investigate the convergence of the proposed two-stage iterative algorithm, and Fig. 3 plots the sum data rate of all CUs $R_{\rm tot}\left(\boldsymbol{\rho},\mathbf{p}^{\rm C},\mathbf{p}^{\rm D}\right)$ versus the number of iterations, where $N=12$, $M=36$. From Fig. 3, we can observe that $R_{\rm tot}\left(\boldsymbol{\rho},\mathbf{p}^{\rm C},\mathbf{p}^{\rm D}\right)$ increases uniformly and converges to the peak value after about 6 iterations. Besides, it can be found that the tradeoff parameter ε and the number of D2D pairs have insignificant influence on the speed of convergence. The observed results also coincide with Theorem 5 given in Section IV.

2) Performance Comparisons: Furthermore, numerical results are presented in Figs. 4-6 to evaluate the performance of our proposed robust scheme in terms of EE, SE and D2D pairs QoS satisfying probability compared to the non-robust scheme. Note that the non-robust scheme indicates that channel uncertainties are not taken into consideration and all the channel estimates are adopted directly as they were accurate. However, the interference channel uncertainties still exist in the non-robust scheme. Particularly, the effective EE and SE are considered in Figs. 4-5, which is set as 0 when the minimum rate requirements of CUs or D2D pairs are not satisfied.

Specifically, the performances of EE and SE are presented with the variation of the tradeoff parameter ε and the normalized error bound $\delta_{\max}$ in Fig. 4 and Fig. 5, respectively. It can be observed in Fig. 4 that for a given ε, the EE under the non-robust scheme decreases rapidly with the increase of $\delta_{\max}$ while the EE under the robust scheme declines slightly with $\delta_{\max}$. This is because when $\delta_{\max}$ increases, the minimum rate requirements of CUs and D2D pairs for the non-robust scheme are more likely to be violated, and the effective EE for non-robust case is treated as 0 to present the infeasibility of the constraint C6. In contrast, as the proposed robust scheme is guaranteed to satisfy the rate requirements of CUs invariably, the EE under our robust scheme is strictly greater than 0 all the time. Similarly, we can also observe from Fig. 5 that for a given ε, a larger $\delta_{\max}$ leads to a worse SE, and the robust scheme achieves higher effective SE in comparison with the non-robust scheme for the same ε and $\delta_{\max}$.

On the other hand, by adjusting the tradeoff parameter ε from 6 to 7.5, Fig. 4 and Fig. 5 also show the tradeoff performance between EE and SE under robust and non-robust schemes. When $\delta_{\max}$ is fixed, the effective SE always increases with ε under both schemes as shown in Fig. 5.

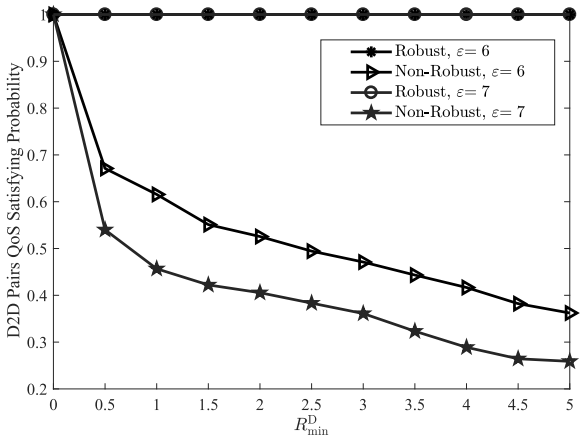

Fig. 7. D2D pairs QoS satisfying probability *vs.* $R^{\mathrm{D}}_{\min}$ for robust and non-robust schemes.

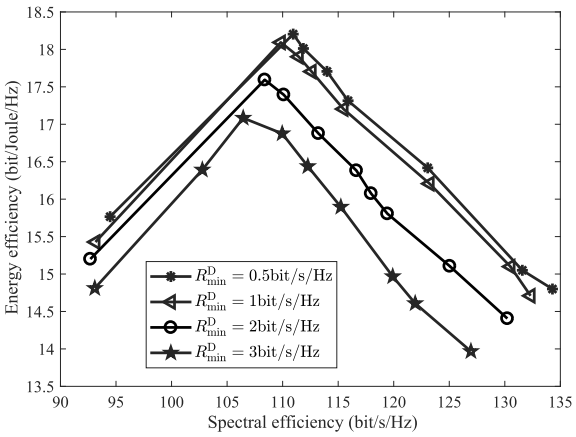

Fig. 8. Energy efficiency *vs.* spectral efficiency with different $R^{\mathrm{D}}_{\min}$ for the proposed robust scheme.

This is because larger ε indicates more transmit power is available to improve the transmission rate of CUs. On the contrary, in Fig. 4, the effective EE first increases and then declines with the growing of ε for both schemes. When ε is small, the power consumption for data transmission plays a small part in the total power consumption compared to the fixed circuit power consumption. Under this circumstance, SE goes up at a higher speed than the whole power consumption, and thus EE also increases with ε until reaching the peak point. After that, the growing of transmit power consumption cannot be neglected, and the increase of SE is slower owing to the reducing gradient of the logarithmic rate-power function. Consequently, EE turns to decrease with ε.

In addition, the QoS satisfying probability of D2D pairs is plotted against ε and $\delta_{\max}$ in Fig. 6. It can be easily found that our proposed robust scheme can always satisfy the minimum rate requirements of all D2D pairs with the variation of ε and $\delta_{\max}$, and therefore its QoS satisfying probability is always 1. In contrast, for the non-robust scheme, the QoS satisfying probability of D2D pairs decreases with both ε and $\delta_{\max}$. Specifically, when ε increases, CUs will transmit data with higher transmit power to improve the system SE, which produces more serious interference to D2D pairs sharing the same RB. Besides, with the increase of $\delta_{\max}$, the deviation range of the interference to D2D pairs extends gradually, which also increases the violation probability of the minimum rate constraint C7.

3) Impact of D2D Minimum Rate Requirement: Fig. 7 and Fig. 8 show the impact of the minimum rate requirements of D2D pairs $R^{\mathrm{D}}_{\min}$ on the D2D pairs QoS satisfying probability and the EE-SE tradeoff. It is readily observed in Fig. 7 that our proposed robust scheme can always satisfy the minimum rate requirements of D2D pairs, while the D2D pairs QoS satisfying probability for the non-robust scheme declines with the increase of $R^{\mathrm{D}}_{\min}$. Besides, for the non-robust scheme, the increase of ε also contributes to the deterioration of QoS satisfying probability for D2D pairs, since higher level of interference from CUs will be imposed on D2D pairs sharing the same RBs. Then, in Fig. 8, as ε increases from 6 to 7.5, higher rate requirement of D2D pairs means worse

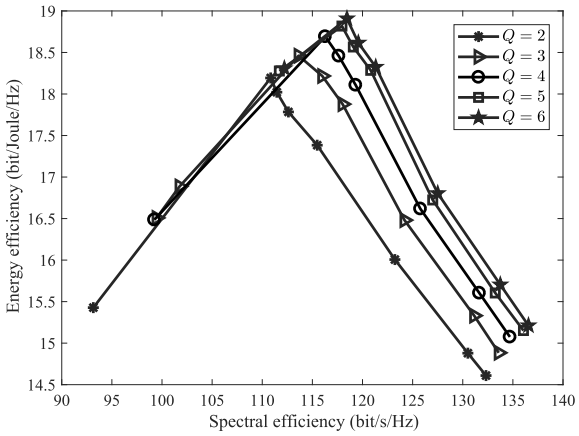

Fig. 9. Energy efficiency *vs.* spectral efficiency with different Q for the proposed robust scheme.

performance in terms of the EE-SE tradeoff. Specifically, for the same EE, the SE is reduced with higher minimum rate requirement of D2D pairs. Since D2D pairs need to transmit with larger power to achieve higher rate, heavier interference will be introduced to the CUs which share the same RBs. Therefore, from Fig. 8, we can conclude that there exists a tradeoff between the rate requirement of D2D pairs and the EE-SE performance of CUs.

4) Effect of RB Quota: To investigate the impact of the maximum number of D2D pairs at each RB, the curves for the tradeoff between EE and SE with different Q are plotted in Fig. 9. With the increasing of ε from 6 to 7.5, all the five curves show the same trend that EE first goes up and then declines with the growing of SE. As shown at the second half of curves where EE declines with the increase of SE, higher SE can be obtained with larger value of Q for the same EE. With the increase of Q, more D2D pairs are permitted to share the same RB, which provides more degrees of freedom in spectrum allocation and thus contributes to the improvement of SE. Besides, when Q increases from 2 to 6, the maximum EE and its corresponding SE first increases and then remains stable, which indicates that allowing five or more D2D pairs to share the same RB cannot obtain extra performance gain.

This is mainly due to the fact that more D2D pairs sharing one RB will also introduce heavier mutual interference, which reduces the performance advantage of spectrum sharing to some extent. Therefore, the maximum EE and corresponding SE cannot be enhanced by increasing the maximum number of D2D pairs at each RB. Also, as the computational complexity of Algorithm 3 rises up with Q, the choice of Q should be appropriate, which is suggested to be 5 for the given simulation settings.

VI. Conclusion

In this paper, the robust multi-objective optimization in D2D communications underlaying HetNets has been investigated, and the uncertain MOO problem was formulated to optimize the system EE and SE at the same time under the minimum rate requirements of all CUs and D2D pairs, where the uncertainties of all interference channels were taken into consideration. Then, we proposed an effective two-stage iterative algorithm for the joint optimization of the spectrum allocation and power coordination with polynomial complexity, whose convergence and optimality were demonstrated through theoretical derivation. Besides, our proposed algorithm converged fast as shown in numerical results. Compared to the non-robust scheme, the proposed robust scheme achieved much higher effective EE and SE, and always satisfied the minimum rate requirements of D2D pairs. By investigating the impact of the D2D pairs' minimum rate requirements, we found there existed an intrinsic tradeoff between the EE-SE performance of CUs and the minimum rate requirements of D2D pairs. Finally, the effect of the RB quota was studied, which suggested that the choice of quota should be appropriate for the compromise between complexity and performance gain.

Appendix A
Proof of Theorem 1

We first prove the sufficiency, and define that

$$\mathbf{F}\left(\mathbf{x}, \mathbf{g}^{\mathrm{C2B}}, \mathbf{g}^{\mathrm{D2B}}\right) = \left[\mathrm{f}_1\left(\mathbf{x}, \mathbf{g}^{\mathrm{C2B}}, \mathbf{g}^{\mathrm{D2B}}\right) \mathrm{f}_2\left(\mathbf{x}\right)\right]^{\mathrm{T}}, \quad (35)$$

where $\mathbf{x} = \left(\boldsymbol{\rho}, \mathbf{p}^{\mathrm{C}}, \mathbf{p}^{\mathrm{D}}\right)$. Assume that $\mathbf{x}^*$ is robust Pareto optimal for $\mathcal{P}\left(\mathcal{G}\right)$, and thus there does not exist $\mathbf{x}$ satisfying $\mathrm{C1}-\mathrm{C7}$ and $\mathbf{F}_{\mathcal{G}}\left(\mathbf{x}\right) - \mathbb{R}^2_{\geq} \subseteq \mathbf{F}_{\mathcal{G}}\left(\mathbf{x}^*\right) - \mathbb{R}^2_{\geq}$ simultaneously.

Suppose that $\mathbf{x}^*$ is not Pareto optimal for problem (16), which indicates that there exists another feasible solution $\mathbf{x}'$ of problem (16) satisfying

$$\mathbf{F}\left(\mathbf{x}', \mathbf{g}^{\mathrm{C2B}}_{\max}\left(\mathbf{x}'\right), \mathbf{g}^{\mathrm{D2B}}_{\max}\left(\mathbf{x}'\right)\right) \in \mathbf{F}\left(\mathbf{x}^*, \mathbf{g}^{\mathrm{C2B}}_{\max}\left(\mathbf{x}^*\right), \mathbf{g}^{\mathrm{D2B}}_{\max}\left(\mathbf{x}^*\right)\right) - \mathbb{R}^2_{\geq}, \quad (36)$$

where

$$\left(\mathbf{g}^{\mathrm{C2B}}_{\max}\left(\mathbf{x}\right), \mathbf{g}^{\mathrm{D2B}}_{\max}\left(\mathbf{x}\right)\right) = \arg \max_{\mathbf{g}^{\mathrm{C2B}}, \mathbf{g}^{\mathrm{D2B}}} \mathrm{f}_1\left(\mathbf{x}, \mathbf{g}^{\mathrm{C2B}}, \mathbf{g}^{\mathrm{D2B}}\right). \quad (37)$$

Since

$$\mathbf{F}\left(\mathbf{x}', \mathbf{g}^{\mathrm{C2B}}, \mathbf{g}^{\mathrm{D2B}}\right) \leq \mathbf{F}\left(\mathbf{x}', \mathbf{g}^{\mathrm{C2B}}_{\max}\left(\mathbf{x}'\right), \mathbf{g}^{\mathrm{D2B}}_{\max}\left(\mathbf{x}'\right)\right), \quad (38)$$

$\forall \mathbf{g}^{\mathrm{C2B}} \in \mathcal{G}^{\mathrm{C2B}}, \mathbf{g}^{\mathrm{D2B}} \in \mathcal{G}^{\mathrm{D2B}}$, always holds, we have

$$\mathbf{F}_{\mathcal{G}}\left(\mathbf{x}'\right) \subseteq \mathbf{F}\left(\mathbf{x}^*, \mathbf{g}^{\mathrm{C2B}}_{\max}\left(\mathbf{x}^*\right), \mathbf{g}^{\mathrm{D2B}}_{\max}\left(\mathbf{x}^*\right)\right) - \mathbb{R}^2_{\geq} \subseteq \mathbf{F}_{\mathcal{G}}\left(\mathbf{x}^*\right) - \mathbb{R}^2_{\geq}, \quad (39)$$

which contradicts with the assumption that $\mathbf{x}^*$ is robust Pareto optimal for $\mathcal{P}\left(\mathcal{G}\right)$. Therefore, $\left(\boldsymbol{\rho}^*, \mathbf{p}^{\mathrm{C}*}, \mathbf{p}^{\mathrm{D}*}\right)$ is Pareto optimal for problem (16) if it is robust Pareto optimal for $\mathcal{P}\left(\mathcal{G}\right)$. Conversely, we can prove the necessity in a similar way, which completes the proof.

Appendix B
Proof of Theorem 2

We first prove the sufficiency. Define that

$$\mathrm{g}_1\left(\mathbf{x}\right) = \max_{\mathbf{g}^{\mathrm{C2B}}, \mathbf{g}^{\mathrm{D2B}}} \mathrm{f}_1\left(\mathbf{x}, \mathbf{g}^{\mathrm{C2B}}, \mathbf{g}^{\mathrm{D2B}}\right), \quad (40a)$$

$$\mathrm{g}_2\left(\mathbf{x}\right) = \mathrm{f}_2\left(\mathbf{x}\right), \quad (40b)$$

where $\mathbf{x} = \left(\boldsymbol{\rho}, \mathbf{p}^{\mathrm{C}}, \mathbf{p}^{\mathrm{D}}\right)$. For given ε, assume $\mathbf{x}^*$ is the unique optimal solution of problem (17), and we have $\mathrm{g}_1\left(\mathbf{x}^*\right) \leq \mathrm{g}_1\left(\mathbf{x}\right)$, for all $\mathbf{x}$ satisfying C1-C5, C6′, C7′ and C8.

Now we suppose that $\mathbf{x}^*$ is not Pareto optimal for the MOO problem (16). Thus, there must exist another solution $\mathbf{x}'$ of problem (17) that satisfies

$$\mathrm{g}_i\left(\mathbf{x}'\right) \leq \mathrm{g}_i\left(\mathbf{x}^*\right), \quad \forall i = 1, 2, \quad (41)$$

and there is at least one $j \in \{1, 2\}$ such that $\mathrm{g}_i\left(\mathbf{x}'\right) < \mathrm{g}_i\left(\mathbf{x}^*\right)$. Apparently, this contradicts with the uniqueness assumption. Therefore, we can conclude that $\mathbf{x}^*$ is Pareto optimal for the MOO problem (16). Furthermore, from Theorem 1, it can be readily obtained that $\mathbf{x}^*$ is also robust Pareto optimal for the original uncertain MOO problem $\mathcal{P}\left(\mathcal{G}\right)$.

On the other hand, it is assumed that $\mathbf{x}^*$ is a robust Pareto optimal solution for problem $\mathcal{P}\left(\mathcal{G}\right)$ and thus Pareto optimal for problem (16). Then, let $\varepsilon = \mathrm{g}_2\left(\mathbf{x}^*\right)$, and suppose that $\mathbf{x}^*$ is not the optimal solution of problem (17). Thus, there must exist another $\mathbf{x}'$ with $\mathrm{g}_1\left(\mathbf{x}'\right) < \mathrm{g}_1\left(\mathbf{x}^*\right)$ and $\mathrm{g}_2\left(\mathbf{x}'\right) \leq \varepsilon = \mathrm{g}_2\left(\mathbf{x}^*\right)$, which contradicts with the assumption that $\mathbf{x}^*$ is Pareto optimal for problem (16). The necessity is also proved.

Appendix C
Proof of Theorem 3

Assuming that $\left(\mathbf{p}^{\mathrm{C},(t)}, \mathbf{p}^{\mathrm{D},(t)}\right)$ is the obtained optimal solution at the t-th iteration, we can obtain that

$$\begin{aligned} R_{\mathrm{tot}}\left(\mathbf{p}^{\mathrm{C},(t-1)}, \mathbf{p}^{\mathrm{D},(t-1)}\right) &\overset{\mathrm{a}}{=} \tilde{R}^{(t)}_{\mathrm{tot}}\left(\mathbf{p}^{\mathrm{C},(t-1)}, \mathbf{p}^{\mathrm{D},(t-1)}\right) \\ &\overset{\mathrm{b}}{\leq} \tilde{R}^{(t)}_{\mathrm{tot}}\left(\mathbf{p}^{\mathrm{C},(t)}, \mathbf{p}^{\mathrm{D},(t)}\right) \\ &\overset{\mathrm{c}}{\leq} R_{\mathrm{tot}}\left(\mathbf{p}^{\mathrm{C},(t)}, \mathbf{p}^{\mathrm{D},(t)}\right), \end{aligned} \quad (42)$$

where the equality (a) is because $Y_n\left(\mathbf{p}^{\mathrm{C},(t-1)}, \mathbf{p}^{\mathrm{D},(t-1)}\right) = \tilde{Y}^{(t)}_n\left(\mathbf{p}^{\mathrm{C},(t-1)}, \mathbf{p}^{\mathrm{D},(t-1)}\right)$; the inequality (b) is valid due the fact that problem (32) is convex and $\left(\mathbf{p}^{\mathrm{C},(t)}, \mathbf{p}^{\mathrm{D},(t)}\right)$ is its global optimal solution; the inequality (c) holds since $\tilde{R}^{(t)}_{\mathrm{tot}}\left(\mathbf{p}^{\mathrm{C}}, \mathbf{p}^{\mathrm{D}}\right)$ is the lower bound of $R_{\mathrm{tot}}\left(\mathbf{p}^{\mathrm{C}}, \mathbf{p}^{\mathrm{D}}\right)$ according to (29). Therefore, $R_{\mathrm{tot}}\left(\mathbf{p}^{\mathrm{C}}, \mathbf{p}^{\mathrm{D}}\right)$ is improved at each iteration.

Besides, as the constraint set is compact and there exists an upper bound of $R_{\mathrm{tot}}\left(\mathbf{p}^{\mathrm{C}}, \mathbf{p}^{\mathrm{D}}\right)$ for the given transmit power budget, Algorithm 1 must converge. Assume $\left(\mathbf{p}^{\mathrm{C}*}, \mathbf{p}^{\mathrm{D}*}\right)$ is

the convergent solution. As the objectives and constraints in problem (23) and problem (32) have the same values and derivative values at $\left(\mathbf{p}^{\mathrm{C}*}, \mathbf{p}^{\mathrm{D}*}\right)$, $\left(\mathbf{p}^{\mathrm{C}*}, \mathbf{p}^{\mathrm{D}*}\right)$ must satisfy the KKT conditions of problem (23).

Appendix D
Proof of Theorem 4

Assume that the τ_{s}-th swap operations is forced by the swap-blocking pair (DP_k, DP_j), i.e., $\mathrm{M}^{(\tau_{\mathrm{s}})} = \mathrm{M}^{(\tau_{\mathrm{s}}-1)}{}_{jl}^{km}$. From the definition of swap-blocking pairs, it can be obtained that

$$\begin{aligned}
&R_{\mathrm{tot}}\left(\mathrm{M}^{(\tau_{\mathrm{s}})}\right) - R_{\mathrm{tot}}\left(\mathrm{M}^{(\tau_{\mathrm{s}}-1)}\right) \\
&= \sum_{n\in\mathcal{C}}\left(R_n^{\mathrm{C}}\left(\mathrm{M}^{(\tau_{\mathrm{s}})}\right) - R_n^{\mathrm{C}}\left(\mathrm{M}^{(\tau_{\mathrm{s}}-1)}\right)\right) \\
&= \sum_{m'\in\mathcal{M}}\left(U_{RB_{m'}}\left(\mathrm{M}^{(\tau_{\mathrm{s}})}\right) - U_{RB_{m'}}\left(\mathrm{M}^{(\tau_{\mathrm{s}}-1)}\right)\right) \\
&= U_{RB_m}\left(\mathrm{M}^{(\tau_{\mathrm{s}})}\right) + U_{RB_l}\left(\mathrm{M}^{(\tau_{\mathrm{s}})}\right) \\
&\quad - U_{RB_m}\left(\mathrm{M}^{(\tau_{\mathrm{s}}-1)}\right) - U_{RB_l}\left(\mathrm{M}^{(\tau_{\mathrm{s}}-1)}\right) \\
&\geq 0, \qquad (43)
\end{aligned}$$

which indicates that the objective function of problem (24) will not decrease with the progress of Algorithm 3. Since the numbers of D2D pairs and RBs are both finite, the number of potential swap operations is also finite. Hence, the convergence of Algorithm 3 must occur in a finite amount of iterations.

As depicted in Algorithm 3, when it converges, no D2D pair can find another D2D pair to constitute a swap-blocking pair. In other words, the matching at convergence is a two-sided exchange-stable matching, which completes the proof.

Appendix E
Proof of Theorem 5

Considering the τ-th iteration of Algorithm 4, we can obtain the following inequality

$$\begin{aligned}
&R_{\mathrm{tot}}\left(\boldsymbol{\rho}^{(\tau-1)}, \mathbf{p}^{\mathrm{C},(\tau-1)}, \mathbf{p}^{\mathrm{D},(\tau-1)}\right) \\
&\quad \overset{\alpha}{\leq} R_{\mathrm{tot}}\left(\boldsymbol{\rho}^{(\tau)}, \mathbf{p}^{\mathrm{C},(\tau-1)}, \mathbf{p}^{\mathrm{D},(\tau-1)}\right) \\
&\quad \overset{\beta}{\leq} R_{\mathrm{tot}}\left(\boldsymbol{\rho}^{(\tau)}, \mathbf{p}^{\mathrm{C},(\tau)}, \mathbf{p}^{\mathrm{D},(\tau)}\right). \qquad (44)
\end{aligned}$$

Specifically, the first inequality α has been verified in Theorem 4 where the sum rate of CUs will not decrease after Algorithm 3 conducted. Also, Theorem 3 has illustrated that $R_{\mathrm{tot}}\left(\mathbf{p}^{\mathrm{C}}, \mathbf{p}^{\mathrm{D}}\right)$ increases with the number of iterations, which proves the second inequality β. Hence, Algorithm 4 monotonically decreases the objective of problem (22) at each iteration. Furthermore, with the given spectrum and power budget, the sum rate of CUs $R_{\mathrm{tot}}\left(\boldsymbol{\rho}, \mathbf{p}^{\mathrm{C}}, \mathbf{p}^{\mathrm{D}}\right)$ is upper bounded. Therefore, Algorithm 4 is guaranteed to converge after finite iterations at either $flag < \Phi$ or $\left|\frac{R_{\mathrm{tot}}\left(\boldsymbol{\rho}^{(\tau)}, \mathbf{p}^{\mathrm{C},(\tau)}, \mathbf{p}^{\mathrm{D},(\tau)}\right) - R_{\mathrm{tot}}\left(\boldsymbol{\rho}^{(\tau-1)}, \mathbf{p}^{\mathrm{C},(\tau-1)}, \mathbf{p}^{\mathrm{D},(\tau-1)}\right)}{R_{\mathrm{tot}}\left(\boldsymbol{\rho}^{(\tau-1)}, \mathbf{p}^{\mathrm{C},(\tau-1)}, \mathbf{p}^{\mathrm{D},(\tau-1)}\right)}\right| < \Phi$.

References

[1] C. Yang, J. Li, M. Guizani, A. Anpalagan, and M. Elkashlan, "Advanced spectrum sharing in 5G cognitive heterogeneous networks," *IEEE Wireless Commun.*, vol. 23, no. 2, pp. 94–101, Apr. 2016.

[2] X. Ge, S. Tu, G. Mao, and C. X. Wang, "5G ultra-dense cellular networks," *IEEE Trans. Wireless Commun.*, vol. 23, no. 1, pp. 72–79, Feb. 2016.

[3] X. Ge, J. Yang, H. Gharavi, and Y. Sun, "Energy efficiency challenges of 5G small cell networks," *IEEE Commun. Mag.*, vol. 55, no. 5, pp. 184–191, May 2017.

[4] F. Malandrino, C. Casetti, and C. F. Chiasserini, "Toward D2D-enhanced heterogeneous networks," *IEEE Commun. Mag.*, vol. 52, no. 11, pp. 94–100, Nov. 2014.

[5] J. Zhao, Y. Liu, K. K. Chai, Y. Chen, and M. Elkashlan, "Joint subchannel and power allocation for NOMA enhanced D2D communications," *IEEE Trans. Commun.*, vol. 65, no. 11, pp. 5081–5094, Nov. 2017.

[6] A. Asadi, Q. Wang, and V. Mancuso, "A survey on device-to-device communication in cellular networks," *IEEE Commun. Surveys Tuts.*, vol. 16, no. 4, pp. 1801–1819, Nov. 2014.

[7] Y. Hao, Q. Ni, H. Li, and S. Hou, "Energy and spectral efficiency tradeoff with user association and power coordination in massive MIMO enabled HetNets," *IEEE Commun. Lett.*, vol. 20, no. 10, pp. 2091–2094, Oct. 2016.

[8] J. B. Rao and A. O. Fapojuwo, "An analytical framework for evaluating spectrum/energy efficiency of heterogeneous cellular networks," *IEEE Trans. Veh. Technol.*, vol. 65, no. 5, pp. 3568–3584, May 2016.

[9] Y. Hao, Q. Ni, H. Li, and S. Hou, "On the energy and spectral efficiency tradeoff in massive MIMO-enabled HetNets with capacity-constrained backhaul links," *IEEE Trans. Commun.*, vol. 65, no. 11, pp. 4720–4733, Nov. 2017.

[10] B. Zhuang, D. Guo, and M. L. Honig, "Energy-efficient cell activation, user association, and spectrum allocation in heterogeneous networks," *IEEE J. Sel. Areas Commun.*, vol. 34, no. 4, pp. 823–831, Apr. 2016.

[11] L. Xu, C. Jiang, Y. Shen, T. Q. S. Quek, Z. Han, and Y. Ren, "Energy efficient D2D communications: A perspective of mechanism design," *IEEE Trans. Wireless Commun.*, vol. 15, no. 11, pp. 7272–7285, Nov. 2016.

[12] G. Fodor, D. D. Penda, M. Belleschi, M. Johansson, and A. Abrardo, "A comparative study of power control approaches for device-to-device communications," in *Proc. IEEE ICC*, Budapest, Hungary, Jun. 2013, pp. 6008–6013.

[13] J. J. M. B. da Silva and G. Fodor, "A binary power control scheme for D2D communications," *IEEE Wireless Commun. Lett.*, vol. 4, no. 6, pp. 669–672, Dec. 2015.

[14] Y. Wu, J. Wang, L. Qian, and R. Schober, "Optimal power control for energy efficient D2D communication and its distributed implementation," *IEEE Commun. Lett.*, vol. 19, no. 5, pp. 815–818, May 2015.

[15] A. Zappone, B. Matthiesen, and E. A. Jorswieck, "Energy efficiency in MIMO underlay and overlay device-to-device communications and cognitive radio systems," *IEEE Trans. Signal Process.*, vol. 65, no. 4, pp. 1026–1041, Feb. 2017.

[16] D. D. Penda, L. Fu, and M. Johansson, "Energy efficient D2D communications in dynamic TDD systems," *IEEE Trans. Commun.*, vol. 65, no. 3, pp. 1260–1273, Mar. 2017.

[17] Y. Jiang, Q. Liu, F. Zheng, X. Gao, and X. You, "Energy-efficient joint resource allocation and power control for D2D communications," *IEEE Trans. Veh. Technol.*, vol. 65, no. 8, pp. 6119–6127, Aug. 2016.

[18] T. D. Hoang, L. B. Le, and T. Le-Ngoc, "Energy-efficient resource allocation for D2D communications in cellular networks," *IEEE Trans. Veh. Technol.*, vol. 65, no. 9, pp. 6972–6986, Sep. 2016.

[19] D. Wu, J. Wang, R. Q. Hu, Y. Cai, and L. Zhou, "Energy-efficient resource sharing for mobile device-to-device multimedia communications," *IEEE Trans. Veh. Technol.*, vol. 63, no. 5, pp. 2093–2103, Jun. 2014.

[20] K. Yang, S. Martin, C. Xing, J. Wu, and R. Fan, "Energy-efficient power control for device-to-device communications," *IEEE J. Sel. Areas Commun.*, vol. 34, no. 12, pp. 3208–3220, Dec. 2016.

[21] A. Asheralieva and Y. Miyanaga, "An autonomous learning-based algorithm for joint channel and power level selection by D2D pairs in heterogeneous cellular networks," *IEEE Trans. Commun.*, vol. 64, no. 9, pp. 3996–4012, Sep. 2016.

[22] K. Zhang, M. Peng, P. Zhang, and X. Li, "Secrecy-optimized resource allocation for device-to-device communication underlaying heterogeneous networks," *IEEE Trans. Veh. Technol.*, vol. 66, no. 2, pp. 1822–1834, Feb. 2017.

[23] I. Alqerm and B. Shihada, "Energy-efficient power allocation in multi-tier 5G networks using enhanced online learning," *IEEE Trans. Veh. Technol.*, vol. 66, no. 12, pp. 11086–11097, Dec. 2017.
[24] Z. Zhou, M. Dong, K. Ota, J. Wu, and T. Sato, "Energy efficiency and spectral efficiency tradeoff in device-to-device (D2D) communications," *IEEE Wireless Commun. Lett.*, vol. 3, no. 5, pp. 485–488, Oct. 2014.
[25] O. Aydin, E. A. Jorswieck, D. Aziz, and A. Zappone, "Energy-spectral efficiency tradeoffs in 5G multi-operator networks with heterogeneous constraints," *IEEE Trans. Wireless Commun.*, vol. 16, no. 9, pp. 5869–5881, Sep. 2017.
[26] C. Yang, J. Li, Q. Ni, A. Anpalagan, and M. Guizani, "Interference-aware energy efficiency maximization in 5G ultra-dense networks," *IEEE Trans. Commun.*, vol. 65, no. 2, pp. 728–739, Feb. 2017.
[27] S. Mallick, R. Devarajan, R. A. Loodaricheh, and V. K. Bhargava, "Robust resource optimization for cooperative cognitive radio networks with imperfect CSI," *IEEE Trans. Wireless Commun.*, vol. 14, no. 2, pp. 907–920, Feb. 2015.
[28] A. Memmi, Z. Rezki, and M.-S. Alouini, "Power control for D2D underlay cellular networks with channel uncertainty," *IEEE Trans. Wireless Commun.*, vol. 16, no. 2, pp. 1330–1343, Feb. 2017.
[29] L. Cao, F. Yao, H. Zhao, and J. Zhang, "Distributed resource allocation for D2D-enabled two-tier cellular networks with channel uncertainties," in *Proc. IEEE ICCS*, Shenzhen, China, Dec. 2016, pp. 1–5.
[30] O. Amin, E. Bedeer, M. H. Ahmed, and O. A. Dobre, "Energy efficiency-spectral efficiency tradeoff: A multiobjective optimization approach," *IEEE Trans. Veh. Technol.*, vol. 65, no. 4, pp. 1975–1981, Apr. 2016.
[31] Z. Song, Q. Ni, K. Navaie, S. Hou, S. Wu, and X. Sun, "On the spectral-energy efficiency and rate fairness tradeoff in relay-aided cooperative OFDMA systems," *IEEE Trans. Wireless Commun.*, vol. 15, no. 9, pp. 6342–6355, Sep. 2016.
[32] A. Zappone and E. Jorswieck, "Energy efficiency in wireless networks via fractional programming theory," *Found. Trends Commun. Inf. Theory*, vol. 11, nos. 3–4, pp. 185–396, 2015.
[33] M. Ehrgott, *Multicriteria Optimization*. Heidelberg, Germany: Springer, 2005.
[34] A. Ben-Tal, L. E. Ghaoui, and A. Nemirovski, *Robust Optimization*. Princeton, NJ, USA: Princeton Univ. Press, 2009.
[35] M. Ehrgott, J. Ide, and A. Schöbel, "Minmax robustness for multi-objective optimization problems," *Eur. J. Oper. Res.*, vol. 239, no. 1, pp. 17–31, Nov. 2014.
[36] B. R. Marks and G. P. Wright, "A general inner approximation algorithm for nonconvex mathematical programs," *Oper. Res.*, vol. 26, pp. 681–683, Jul. 1978.
[37] A. Zappone, E. Björnson, L. Sanguinetti, and E. Jorswieck, "Globally optimal energy-efficient power control and receiver design in wireless networks," *IEEE Trans. Signal Process.*, vol. 65, no. 11, pp. 2844–2859, Jun. 2017.
[38] S. Boyd and L. Vandenberghe, *Convex Optimization*. Cambridge, U.K.: Cambridge Univ. Press, 2004.
[39] E. Bodine-Baron, C. Lee, A. Chong, B. Hassibi, and A. Wierman, "Peer effects and stability in matching markets," in *Proc. Algorithmic Game Theory*, 2011, pp. 117–129.

Yuanyuan Hao received the B.Sc. degree in information engineering from the Beijing Institute of Technology, Beijing, China, in 2014, where she is currently pursuing the Ph.D. degree with the School of Information and Electronics. From 2016 to 2017, she was a Visiting Student with the InfoLab21, School of Computing and Communications, Lancaster University, Lancaster, U.K. Her research interests include radio resource management, green communication, multi-tier heterogeneous networks, and massive MIMO and D2D communication.

Qiang Ni (M'04–SM'08) received the B.Sc., M.Sc., and Ph.D. degrees from the Huazhong University of Science and Technology, China, all in engineering. He is currently a Professor and the Head of the Communication Systems Group, School of Computing and Communications, Lancaster University, Lancaster, U.K. His main research interests lie in the area of future generation communication and networking, including green communication and networking, cognitive radio network systems, heterogeneous networks, 5G, SDN, cloud networks, energy harvesting, wireless information and power transfer, IoTs, cyber physical systems, machine learning, big data analytics, and vehicular networks. He has authored or co-authored over 200 papers in these areas.

Hai Li (M'05) received the B.Sc. and Ph.D. degrees from the Beijing Institute of Technology, Beijing, China, in 1997 and 2002, respectively. He is currently an Associate Professor with the School of Information and Electronics, Beijing Institute of Technology. His research interests include signal processing, protocol engineering, and wireless communication.

Shujuan Hou received the B.Sc., M.Sc., and Ph.D. degrees from the Beijing Institute of Technology, Beijing, China, all in signal and information processing. She is currently an Associate Professor with the School of Information and Electronics, Beijing Institute of Technology. Her main research interests are digital signal processing and radio resource management in wireless communication.